HELSINKI UNIVERSITY OF TECHNOLOGY

Department of Civil and Environmental Engineering

MD. MAMUNUL HASSAN

DEFORMATION BEHAVIOUR AND PERMEABILITY OF SOFT FINNISH CLAY

Master's Thesis submitted on 24/01/2006

SUPERVISOR: **Professor PAULI VEPSÄLÄINEN**

INSTRUCTOR: **Lis.Sc (Tech) MATTI LOJANDER**

ABSTRACT OF THE MASTER'S THESIS

HELSINKI UNIVERSITY OF TECHNOLOGY
DEPARTAMENT OF CIVIL AND ENVIROMENTAL ENGINEERING

Author: Md. Mamunul Hassan

Thesis: Deformation behaviour and permeability of soft Finnish clay

Date: 24/01/ 2006 **Number of pages**: 62 p + app. 24p

Chair: Soil Mechanics and Foundation Engineering **Code:** Rak-50

Supervisor: Professor Pauli Vepsäläinen

Instructor: Lis.Sc. (Tech) Matti Lojander

Construction on natural soft soil deposits is still a challenge in geotechnical engineering. It gains even more importance as urban areas all over the world become more and more congested. For socio-economic development today's construction projects are frequently built in those areas, which were considered unsuitable for construction work a couple of decades ago.

Toukoranta is situated in the eastern part of Helsinki near to the outlet of river Vantaa. The area was favoured for dwelling purposes by The City of Helsinki from the early eighties as it is near to the downtown of Helsinki. The original ground level was below sea more than 1 meter. The area was considered completely unsuitable for building purposes because of underlain soft soils, thereby served mainly as filling area. The City of Helsinki fully reclaimed the area by placing filling material over frozen sea in 1985. At the end of 1995 The City of Helsinki constructed a test embankment and an adjacent excavation to study the area. Finite element analyses were performed using Mohr-Coulomb model. Horizontal movements were measured from November 1995 to February 1996. This thesis is also based on finite element method using Mohr-Coulomb and Soft Soil Creep model. Long-term and short-term vertical and horizontal deformation have been analysed. Short-term horizontal movement agreed fairly well to the observed horizontal movement.

Accurate determination of the consolidation and permeability has important economic consequences. The second objective of this work is laboratory determination of horizontal permeability of soft Finnish clay. Most natural soft-clay deposits are more-or-less anisotropic with respect to their flow properties. Typically, the horizontal permeability or flow is higher than that for flow in the vertical direction. Therefore, when horizontal flow predominates, vertical drains generally give an additional benefit to time-settlement behaviour. An oedometer has been developed with vertical drain (VD) in the Laboratory of Soil Mechanics and Foundation Engineering, Helsinki University of Technology, to take account the consolidation or time-settlement behaviour based on horizontal flow. Description of that oedometer and horizontal permeability results are presented.

TEKNILLINEN KORKEAKOULU
RAKENNUS-JA YMPÄRISTÖTEKNIIKAN OSASTO

DIPLOMITYÖN TIIVISTELMÄ

Tekijä: Md. Mamunul Hassan

Diplomityö: Pehmeän saven muodonmuutokset ja vedenläpäisevyys

Päivämäärä: 24/01/ 2006 **Sivumäärä**: 62p+app24p

Professuuri: Pohjarakennus ja maamekaniikka **Koodi:** Rak-50

Valvoja: Professor Pauli Vepsäläinen

Ohjaaja: Lis.Sc. (Tech) Matti Lojander

Rakentaminen heikosti kantavan pehmeän saven varaan on yhä haaste geoteknisille suunnittelijoille. Tiheästi asutuilla alueilla joudutaan nykyisin entistä enemmän rakentamaan alueille, joita ennen pidettiin rakentamiseen sopimattomina.

Toukoranta sijaitsee itäisessä Helsingissä lähellä Vantaan joen suuta. Alue havaittiin 1980-luvulla sopivaksi asutukselle, koska sen sijainti on niin edullinen lähellä Helsingin keskustaa. Alkuperäinen maanpinta oli n. 1m merenpinnan alapuolella. Aluetta oli pidetty sopimattomana rakentamiseen paksujen pehmeiden maakerrosten takia ja siksi aluetta käytettiin lähinnä täyttöalueena. Helsingin kaupunki valtasi maan käyttöön täyttämällä alueen jäälle ajetun hiekan avulla 1985.

Vuoden 1995 lopussa Helsingin kaupunki teki alueelle koerakenteen, jossa oli matala penger ja kaivanto n. 20 m etäisyydellä toisistaan lähinnä sivusiirtymien tutkimista varten. Rakenteen käyttäytymistä mitattiin 3kk ajan marraskuusta 1995 helmikuuhun 1996. Tässä työssä on rakenteen käyttäytymistä analysoitu elementtimenetelmällä käyttäen Mohr-Coulombin mallia sekä myös sekundaaripainuman laskennan sisältävää pehmeän saven mallia. Vaiheittaisen rakentamisen johdosta on jouduttu tarkastelemaan sekä lyhytaikaista että pitkäaikaista käyttäytymistä. Koerakenteen mitatut ja lasketut sivusiirtymät vastaavat hyvin toisiaan.

Työn toisena osana oli saven vedenläpäisevyyden - ennen kaikkea vaakasuuntaisen vedenläpäisevyyden-määrittäminen laboratoriossa. Maan vaakasuuntainen vedenläpäisevyys on usein moninkertainen pystysuuntaiseen verrattuna. Työn yhteydessä kehitettiin ödömetrilaitteella tehtävää pystyojalla varustettua läpäisevyyskoetta. Työssä on esitetty laite- ja koejärjestelyt sekä mittaustuloksia.

PREFACE

I would like to thank Professor Pauli Vepsäläinen, Professor Olli Ravaska, and Lis.Sc. (Tech.) Matti Lojander for teaching, guidance, advice, time and giving me this opportunity to work on this research project. I would also like to thank The City of Helsinki and Fundus for all their support.

Learning PLAXIS was made relatively easy by Jonni Takala. I would like to thank him for teaching me PLAXIS, for his valuable comments, advice, and time. Sometimes hard, sometimes time consuming and sometimes tiresome laboratory tests were converted fun and easy by Jarmo Vihervuori, Matti Ristimäki, Toivo Lemetti. I would like to thank them for their support from the beginning. Also, I thank all other researchers at the Soil Mechanics and Foundation Engineering Laboratory.

Espoo, January 2006

Md. Mamunul Hassan

LIST OF SYMBOLS

Cl-%	Clay content
e	Void ratio
Hm-%	Organic content, %
K_0	Coefficient of the earth pressure at rest
k	Coefficient of permeability, m/s
k_1	Coefficient of permeability at initial state, m/s
n	Porosity, %
OCR	Overconsolidation ratio
p	Mean stress, kPa
p’	Mean effective stress, kPa
q	Deviator stress, kPa
S_r	Degree of Saturation, %
S_t	Sensitivity
u_w	Pore water pressure, kPa
v	Specific Volume
w	Water content, %
w_L	Liquid Limit, %
w_P	Plastic Limit, %
z	Depth, m
σ_v	Reference pressure of Tangent modulus method, 100 kPa
m	Modulus number, Tangent modulus method
β	Stress exponent, Tangent modulus method
λ	Slope of the normal compression line in ln p’ : v plane
κ	Slope of the swelling line in ln p’ : v plane

γ	Unit weight, kN/m^3
γ_w	Unit weight of water, kN/m^3
φ'	Effective friction angle, °
ψ	Dilatancy angle, °
ν	Poisson ratio
E	Young's modulus
c	Cohesion
σ_p	Preconsolidation pressure, kPa
σ'_1,σ'_3	Principal effective stresses, kPa
ε	Strain
POP	Pre-overburden pressure
M_t	Tangent modulus, kPa
M_s	Secant modulus, kPa
M	Slope of Critical State line
c_v	Coefficient of consolidation (vertical flow), m^2/s
c_h	Coefficient of consolidation (horizontal flow), m^2/s
kPa	kN/m^2
r_k	Permeability ratio k_h / k_v
θ	Lode angle, °

TABLE OF CONTENTS

1. INTRODUCTION

Construction on natural soft soil deposits is still a challenge in geotechnical engineering. It gains even more importance as urban areas all over the world become more and more congested. For socio-economic development today's construction projects are frequently built on those areas, which were considered unsuitable for construction work a couple of decades ago.

Toukoranta is situated in the eastern part of Helsinki near to the outlet of river Vantaa. That area was favoured for dwelling purposes by The City of Helsinki from the early eighties as the area is near to the downtown of Helsinki. The original ground level was below more than 1 meter of sea. The area was considered completely unsuitable for building purposes because of underlain soft soils, thereby served mainly as filling area. The City of Helsinki fully reclaimed the area by placing filling material over frozen sea in 1985 (Leppänen 1989).

At the end of 1995 The City of Helsinki constructed a test embankment and an adjacent excavation to study the area. Site investigations and laboratory testing were conducted before construction. The thickness of the deposit was found more than 20 meters. Soil layers were divided into five layers having different thickness. That study was simulated with finite element program, PLAXIS, using Mohr-Coulomb model. The area was well instrumented with inclinometer for three months at various locations around that test embankment and excavation and horizontal displacements were measured (Gulin and Wikström 1997).

The City of Helsinki again took an initiative to study that area in 2004. First objective of this work is to analyse the deformation behaviour. Finite element program PLAXIS is used for simulation. Methodology used to determine soil parameters are described in Chapter 2. Mohr-Coulomb and Soft Soil Creep model are used for finite element simulations. Model parameters of Mohr-Coulomb and Soft Soil Creep model are presented in Chapter 3. Chapter 4 consists of site investigation, laboratory test results, initial information about geometry of the studied area, geological condition, and the test embankment-excavation dimensions. Finite element simulation results and discussion are presented in Section 4.5 of Chapter 4.

The second objective of this work is to study horizontal permeability of soft Finnish clay. Generally, horizontal permeability or flow is higher than that for flow in the vertical direction. Therefore, when horizontal flow predominates, vertical drains generally give an additional benefit to time-settlement behaviour. Accurate determination of the consolidation and permeability has important economic consequences. Methods of laboratory determination of horizontal permeability are presented in Section 5.2. In the Laboratory of Soil Mechanics and Foundation Engineering, Helsinki of University of Technology, an oedometer is especially modified with vertical drain (VD) to take account the effects of consolidation based on horizontal permeability. Description and discussion of that modified oedometer are described in Section 5.3.

2. STRESS-STRAIN-TIME BEHAVIOUR OF SOFT CLAY

2.1 Oedometer test

Calculation of settlements is usually based on the results from oedometer test. The conventional test procedure with incremental loading, each increment being equal to the previous load and a new increment every 24 hours, was suggested by Terzaghi in 1925 and has been widely used since then. During the test, the sample is drained from both ends and readings of the compression are taken in a time sequence enabling a plot of the time-settlement curve for each increment. The results from incremental oedometer tests are usually presented in a diagram where the strain at the end of each step is plotted against logarithm / natural logarithm of vertical effective pressure.

2.1.1 Compression and Recompression index

The deformation parameter for compression index in normally consolidated (NC) part is compression index C_c and in over-consolidated (OC) part the parameter is recompression index C_r. The most typical stress-strain relationship is between the void ratio (e) or specific volume (v) and the vertical effective stress (σ'), obtained from the oedometer test and which can be expressed as a straight line in a semi-logarithmic scale. The relationship is expressed by the Equation (2.1):

$$e = e_0 - C_c \cdot \log_{10} \cdot \frac{\sigma'}{\sigma_0'} \quad \text{.....(2.1)}$$

where, e_0 is the void ratio corresponding to any convenient value of the effective stress σ'_0 and C_c is the compression index.

The same definition applies to the recompression index C_r at the unloading or reloading line.

Slope of the normal compression line or recompression respectively λ and κ can be derived from the oedometer test (Fig 2.1), which have the same slope as C_c and C_r. The difference is that C_c and C_r are plotted in a common-logarithmic scale but λ and κ

are plotted in natural logarithmic scale. So the relationship can be expressed by the following Equations (2.2 and 2.3).

$$\lambda = \frac{C_c}{\ln 10} \quad \text{.....(2.2)}$$

$$\kappa = \frac{C_r}{\ln 10} \quad \text{.....(2.3)}$$

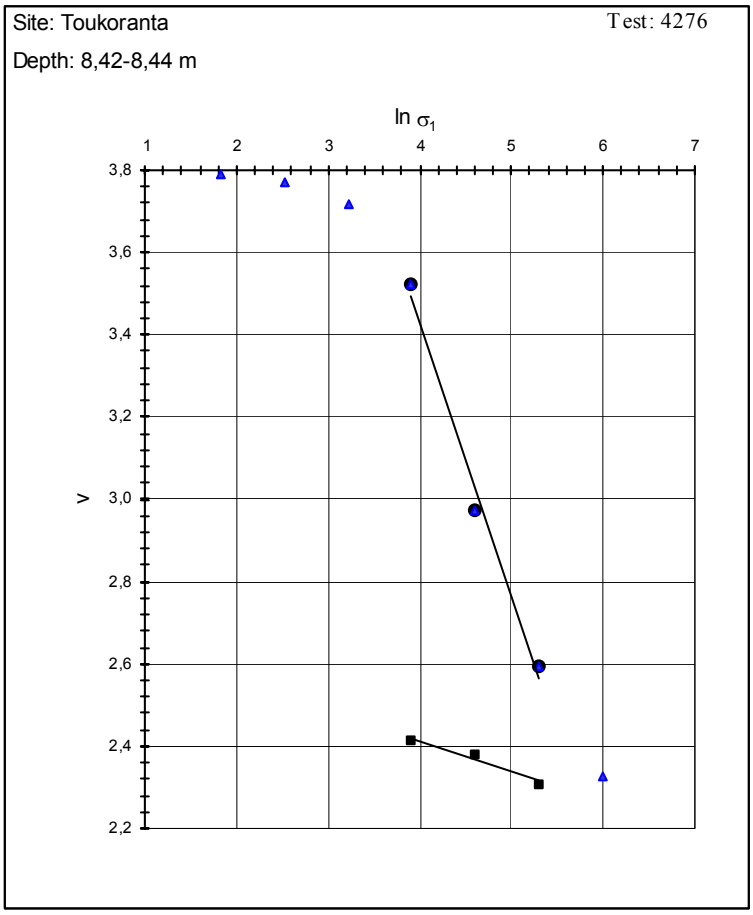

Figure 2.1: *Slope of normal compression line λ and recompression line κ*

2.1.2 Tangent modulus method

Clays in Nordic countries are mainly very soft and young. The assumption, that the oedometer stress-strain relation should be straight line in semi-logarithmic scale (Fig. 2.1) is valid for a small stress range. Therefore, Soil compressibility is expressed by tangent modulus concept expressed by the Equation 2.4, developed by Ohde (1939)-Janbu (1967).

$$M_t = \frac{d\sigma'_1}{d\varepsilon_1} = m\sigma_v \left(\frac{\sigma'_1}{\sigma_v} \right)^{1-\beta} \quad \text{.....(2.4a)}$$

$$\varepsilon_1 = \frac{1}{m\beta} \left[\left(\frac{\sigma'_1}{\sigma'_v} \right)^{\beta} \right] + C_1 \text{ for } \beta \neq 0 \text{ .....(2.4b)}$$

$$\varepsilon_1 = \frac{1}{m} \ln \left(\frac{\sigma'_1}{\sigma'_v} \right) + C_2 \text{ for } \beta = 0 \text{ .....(2.4c)}$$

where,

M_t	Tangent modulus, kPa
m	modulus number
β	stress exponent
σ_1'	effective vertical stress, kPa
σ_v'	reference stress (100kPa)
C_1, C_2	constants
ε_1	relative compression

For normally consolidated line (NC) Janbu's model parameter are expressed as m_1 and β_1. For overconsolidated part the model parameters are expressed as m_2 and β_2.

The C_c model (β=0) is only one special case of this model and in the case of a linear e-logσ graph the following correspondence exists:

$$m = \frac{2.303 \cdot (1 + e_0)}{C_c} \text{ .....(2.4d)}$$

An example of graphic with this model is shown in the following Fig 2.2.

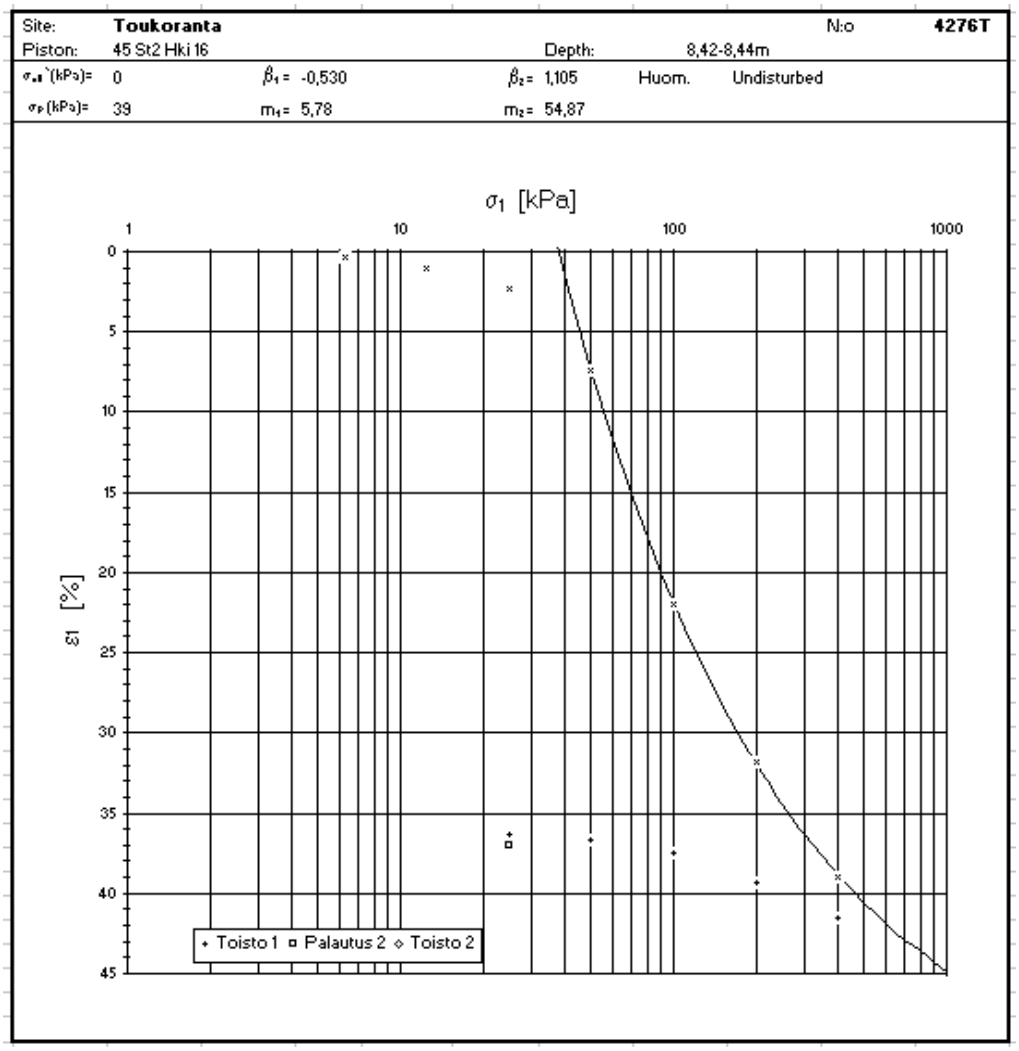

Figure 2.2: *Strain-stress relationship based on Tangent modulus method.*

2.1.3 Coefficient of secondary compression C_α / $C_{\alpha e}$

Time-settlement curves for each load increment are plotted with deformation versus the logarithm of times. The coefficient of secondary compression can be evaluated from the slope of the time-settlement curve after the excess pore pressure dissipation or primary consolidation (Buisman, 1936) (Fig 2.3).

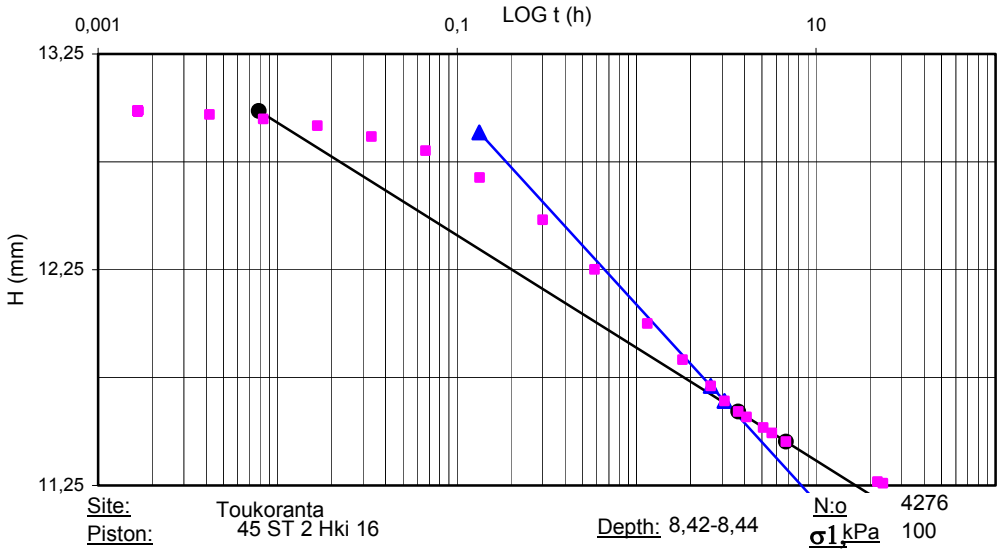

Figure 2.3*: Deformation versus logarithm of time for a load increment*

The coefficient of secondary compression is expressed by the Equation (2.5):

$$C_{\alpha\varepsilon} = \frac{d\varepsilon}{d\log t} \quad \text{.....(2.5a)}$$

$$C_{\alpha} = \frac{de}{d\log t} \quad \text{.....(2.5b)}$$

$$C_{\alpha\varepsilon} = \frac{C_{\alpha}}{1+e_0} \quad \text{.....(2.5c)}$$

The coefficient of secondary compression is not a constant parameter and varies depending on the stress level (Fig 2.4). Generally, below preconsolidation pressure $C_{\alpha\varepsilon}$ values are small. Around preconsolidation pressure, very often, typical reversed s-shaped curve is hard to draw, to obtain the parameter. After preconsolidation pressure reversed s-shape curve can be drawn, thus the coefficient of secondary compression. The empirical relation between the coefficient of secondary compression and relative compression is shown in Fig 2.5.

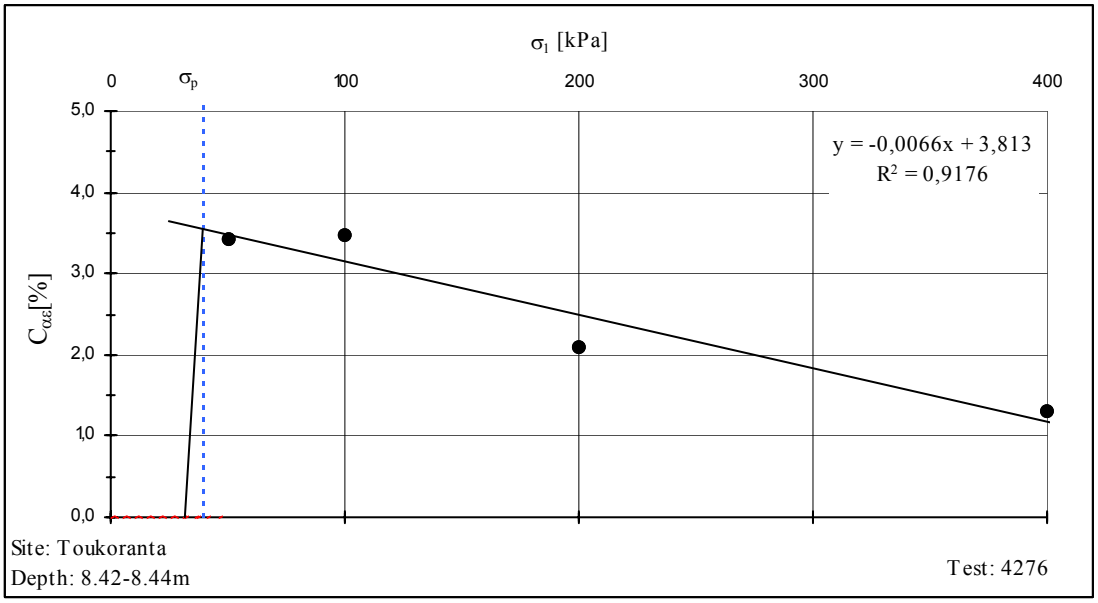

Figure 2.4: *Coefficient of secondary compression versus effective stresses*

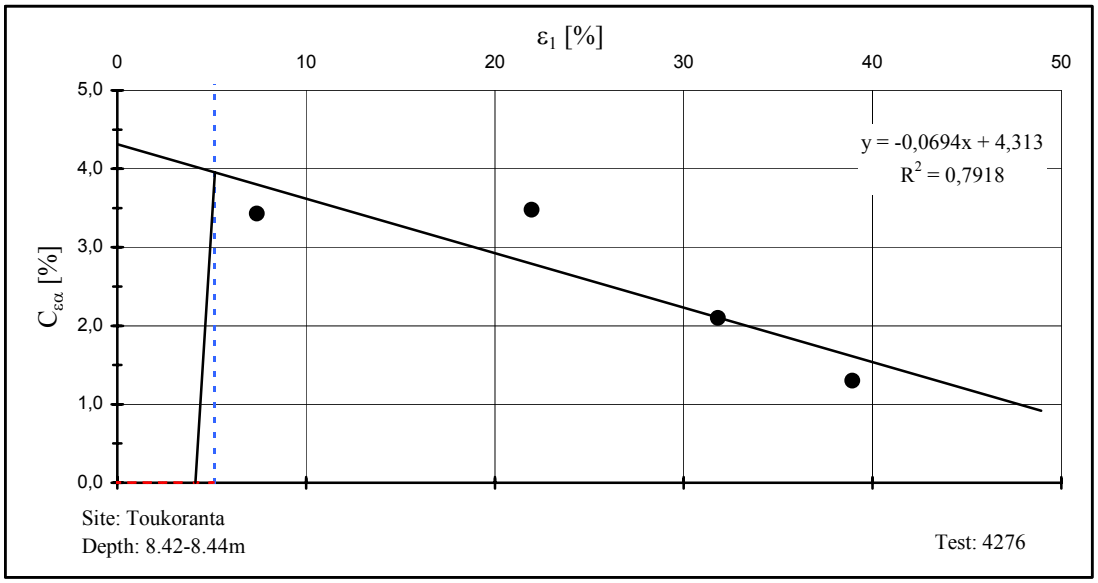

Figure 2.5: *Coefficient of secondary compression versus relative compression*

In Fig 2.4 and Fig 2.5, it is shown that the coefficient of secondary compression is low until a certain pressure, after that it increases rapidly to a maximum value and then slowly decreases. The critical pressure where $C_{\alpha\varepsilon}$ starts to increase corresponds to an effective vertical stress of about $0.8\sigma_p$ for clay (Larsson, 1981).

2.1.4 Coefficient of consolidation c_v

In primary consolidation, the coefficient of consolidation c_v , plays an important role. According to Terzaghi's consolidation theory, it is be expressed by the following equation

$$c_v = \frac{k \cdot M_s}{\gamma_w} \quad \text{.....(2.6)}$$

where k is the coefficient of permeability, M_s is the secant modulus and γ_w is the unit weight of water.

The coefficient of consolidation is not an intrinsic property of soil but the product of deformation modulus M and coefficient of permeability k. It is assumed that both these parameter are constants thus the coefficient of consolidation. It is evident that k decreases with increasing stress as the volume of the pore network in the soil decreases and M increases with increasing stress (Ravaska & Vepsäläinen, 2001).

Generally, coefficient of consolidation c_v is determined from oedometer test results using either Taylor's or Casagrande's curve fitting method (Fig 2.6 & 2.7) for each loading step.

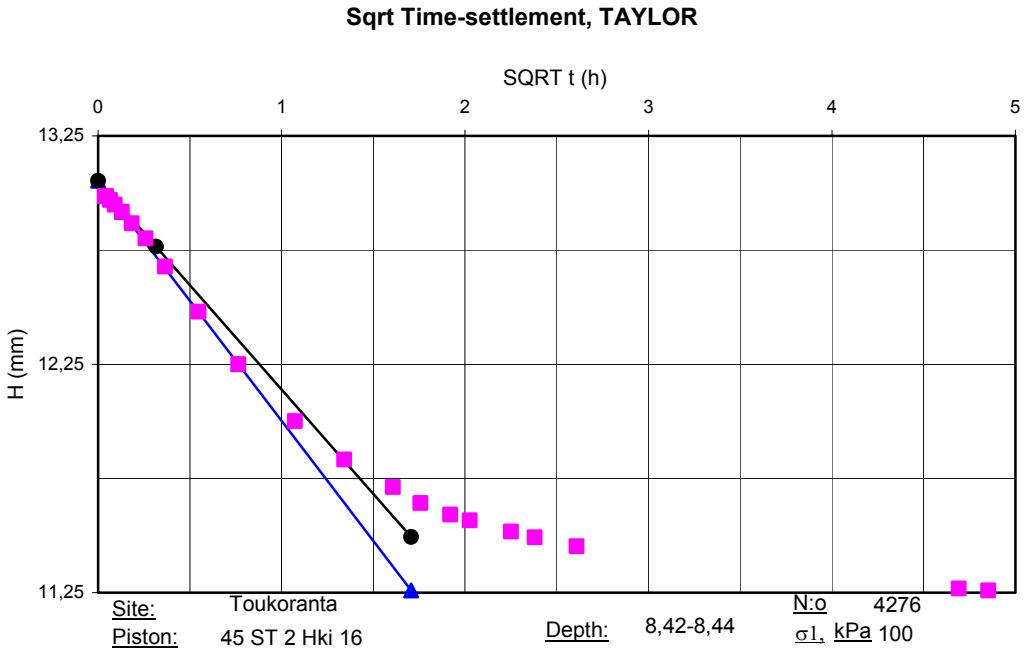

Figure 2.6: *Deformation versus $t^{1/2}$ to calculate t_{90} in Taylor's method.*

The coefficient of consolidation c_v can be obtained using Taylor's method by the following equation (Scott, 1980, 114-117 p):

$$c_v = 0{,}848 \cdot \frac{d^2}{t_{90}} \quad \text{.....(2.7)}$$

where, d is the length of the maximum drainage path, t_{90} is the time of 90 % of consolidation.

In Casagrande's method, the settlement is plotted against the logarithm of time (Fig 2.7) and coefficient of consolidation c_v can be obtained using Equation (2.8)

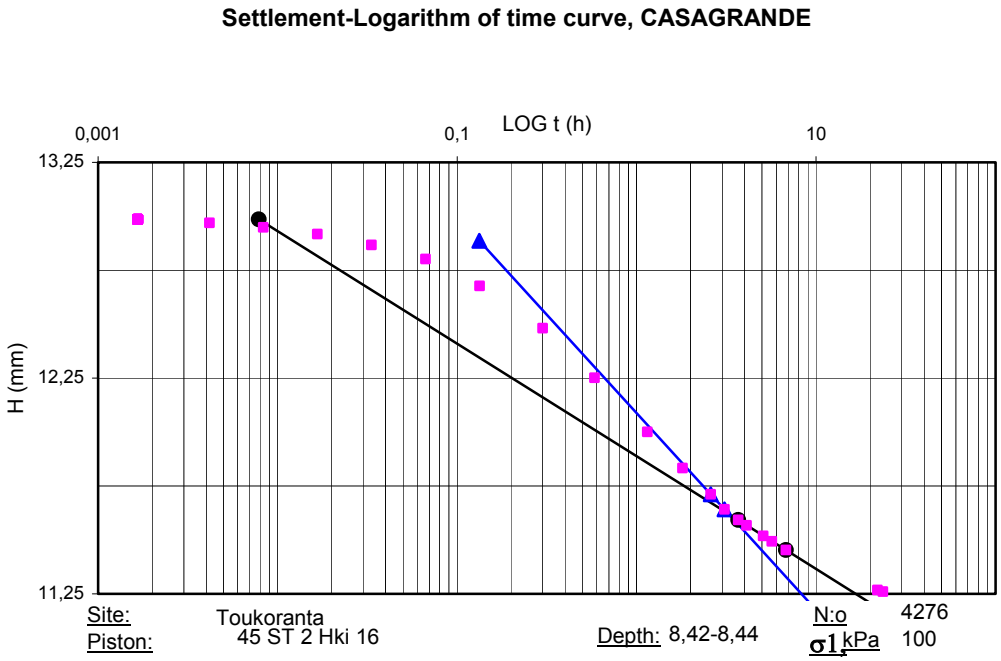

Figure 2.7: *Deformation-log (t) to calculate t_{50} in Casagrande's method*

$$c_v = 0.196 \cdot \frac{d^2}{t_{50}} \quad \text{.....(2.8)}$$

where, d is the length of the maximum drainage path, t_{50} is the time of 50 % of consolidation.

2.1.5 Coefficient of permeability *k*

Permeability has a significant influence on the consolidation characteristics of soil. Coefficient of permeability *k* can be evaluated indirectly from coefficient of consolidation (Equation 2.9) using Taylor's or Casagrande's method for each load step.

$$k = \frac{c_v \cdot \gamma_w}{M_s} \quad \text{.....(2.9)}$$

To evaluate the initial coefficient of permeability k_i, it is assumed that logarithm *k* versus relative compression curve becomes straight after presonsolidation pressure. The initial coefficient of permeability k_i is determined from the intersection of the straight line of logarithm *k*–relative compression curve and the horizontal line of strain representing preconsolidation strain. After the initial coefficient of permeability k_i, decrease in permeability with compression is expressed by the following Equation (2.10). Fig 2.8 shows log*k*–relative compression curve, where coefficient of permeability *k* can be determined using both Taylor's or Casagrande's method.

$$\beta_k = -\frac{\Delta \log k}{\Delta \varepsilon} \quad \text{.....(2.10)}$$

where β_k is the slope of the coefficient of permeability and relative compression in semi-logarithmic plot.

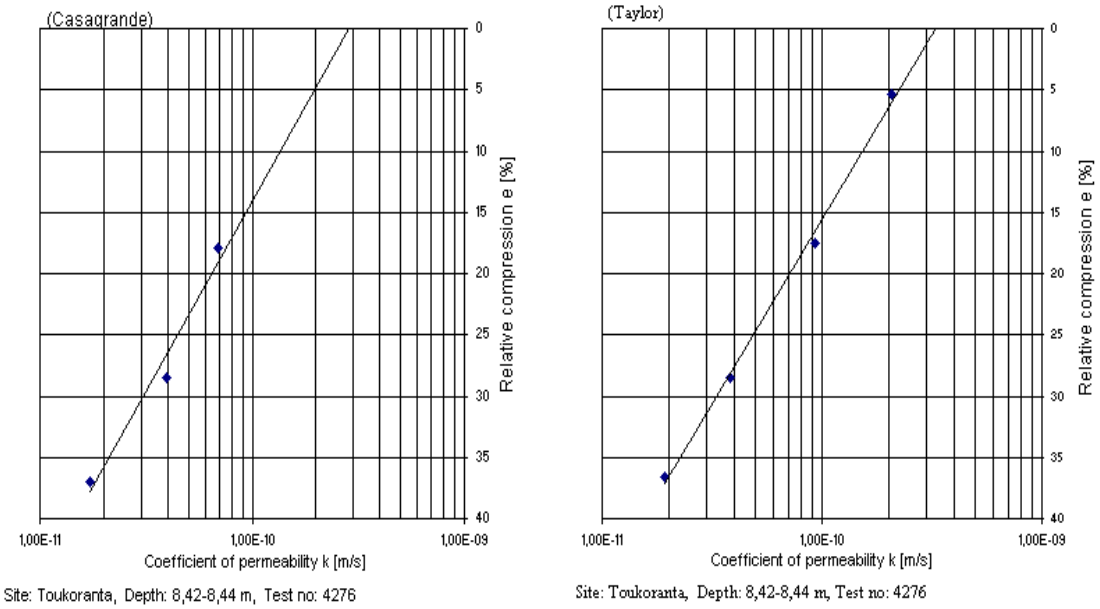

Figure 2.8: *Coefficient of permeability versus relative compression (Casagrande's and Taylor's method)*

2.1.6 Direct determination of coefficient of permeability *k*

Direct determination of coefficient of permeability *k* can also be performed using modified oedometer because normally coefficient of permeability *k* of clay is below 10^{-7} m/s. Indirect evaluation of coefficient of permeability *k* from time-settlement curve are often lower than the direct measurement. Oedometers can be modified to enable direct measurement of coefficient of permeability *k* at different stages of test suggested by Tavenas *et. al*. (1983). This procedure follows falling permeability test method and coefficient of permeability can be determined by the Equation 2.11.

$$k = 2.30 \cdot \frac{a \cdot L}{A} \cdot \frac{1}{t_2 - t_1} \cdot \log\left(\frac{h_1}{h_2}\right) \quad \text{.....(2.11)}$$

where a is the cross-sectional of the tube, A is the cross-sectional area of the sample of height L and t_1 and t_2 are the times at which heads h_1 and h_2 are measured in the tube.

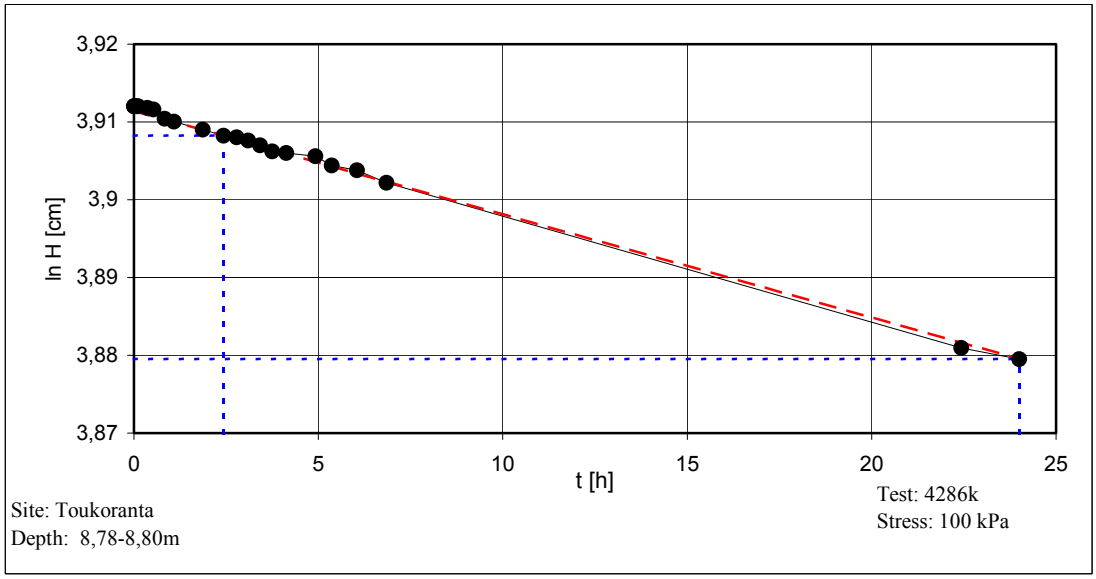

Figure 2.9: *Graphic ln(H)-t to calculate coefficient of permeability*

To evaluate the initial coefficient of permeability k_i and β_k the same procedure described in Section 2.1.6 is used.

2.2 Triaxial test

Generally, strength of soil is represented by Mohr-Coulomb failure criteria. According to this failure condition failure of a soil mass will occur if the shear stress reaches a critical value (Equation 2.12) (Fig. 2.10).

$$\tau = c' + \left(\sigma' \tan \phi'\right) \quad \text{.....(2.12)}$$

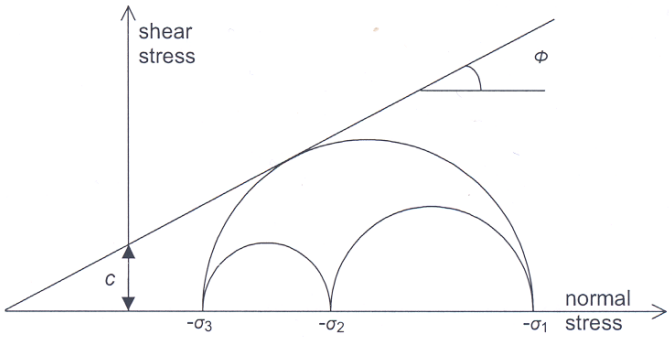

Figure 2.10: *Mohr-Coulomb failure criteria (compression negative)*

Triaxial test are frequently used to evaluate strength parameters of soil. Generally effective stress and shear stress are in triaxial stress space represented by the Equations 2.13-2.16 (Roscoe *et.al.* 1958).

$$p' = \frac{1}{3}\left(\sigma'_{xx} + \sigma'_{yy} + \sigma'_{zz}\right) = \frac{1}{3}\left(\sigma'_1 + \sigma'_2 + \sigma'_3\right) \quad \text{.....(2.13)}$$

$$q = \sqrt{\frac{1}{2}\left(\left(\sigma'_{xx} - \sigma'_{yy}\right)^2 + \left(\sigma'_{yy} - \sigma'_{zz}\right)^2 + \left(\sigma'_{zz} - \sigma'_{xx}\right)^2 + 6\left(\sigma^2{}_{xy} + \sigma^2{}_{yz} + \sigma^2{}_{zx}\right)\right)} \quad \text{.....(2.14)}$$

where *p'* is the isotropic effective stress, or mean effective stress, and *q is* the equivalent shear stress.

For triaxial stress states, where $\sigma'_2 = \sigma'_3$, the mean effective stresses, shear stress and Lode angel θ are expressed by the following Equations.

$$p' = \frac{1}{3}\left(\sigma'_1 + 2\sigma'_3\right) \quad \text{.....(2.15)}$$

$$q = \left|\sigma_1' - \sigma_3'\right| \quad \text{.....(2.16)}$$

$$\theta = \tan^{-1}\left[\frac{\sigma_1 - 2\sigma_3 + \sigma_3}{\sqrt{3(\sigma_1 - \sigma_3)}}\right] \quad \text{.....(2.17a)}$$

or,

$$\theta = 30° \quad \text{.....(2.17b)}$$

2.2.1 Critical state for natural clays

Elastic-plastic model, Cam clay (Roscoe and Schofield 1963) and later Modified Cam Clay (Roscoe and Burland 1968), expresses the ultimate condition in which plastic shearing could continue indefinitely without changes in volume or effective stresses. This perfect plasticity condition implies that cohesive strength becomes zero ($c' = 0$) and soil behaves like a pure frictional manner.

Critical state is evaluated in drained or undrained triaxial tests by Equation 2.18 and 2.19 respectively

$$\frac{\partial p'}{\partial \varepsilon} = \frac{\partial q}{\partial \varepsilon} = \frac{\partial v}{\partial \varepsilon} \quad \text{.....(2.18)}$$

$$\frac{\partial p'}{\partial \varepsilon} = \frac{\partial q}{\partial \varepsilon} = \frac{\partial u}{\partial \varepsilon} \quad \text{.....(2.19)}$$

Thus the stress ratio in critical state can be expressed by the Equation 2.20

$$\frac{q_{cs}}{p'_{cs}} = \eta_{cs} = M \quad \text{.....(2.20)}$$

To evaluate friction angel from critical state of soils Equation 2.12 is converted in terms of principal stresses to Equation 2.21

$$\frac{\sigma_1' + c' \cot \phi'}{\sigma_3' + c' \cot \phi'} = \frac{1 + \sin \phi'}{1 - \sin \phi'} \quad \text{.....(2.21)}$$

Equation 2.21 can also be expressed in terms of triaxial stress variable (Equation 2.15 and 2.17) and becomes

$$\frac{q}{p' + c' \cot \phi'} = \frac{3 \sin \phi'}{\sqrt{3} \cos \theta - \sin \theta \sin \phi'} \quad \text{.....(2.22)}$$

For critical state, as soil behaves pure frictional manner and cohesive strength becomes zero, from Equation 2.23 friction angle can be evaluated. Fig 2.11 shows stress path of to evaluate critical state line.

$$M_{com} = \frac{6 \sin \phi'}{3 - \sin \phi'} \quad \text{.....(2.23)}$$

or,

$$\sin \phi' = \frac{3M}{6 + M}$$

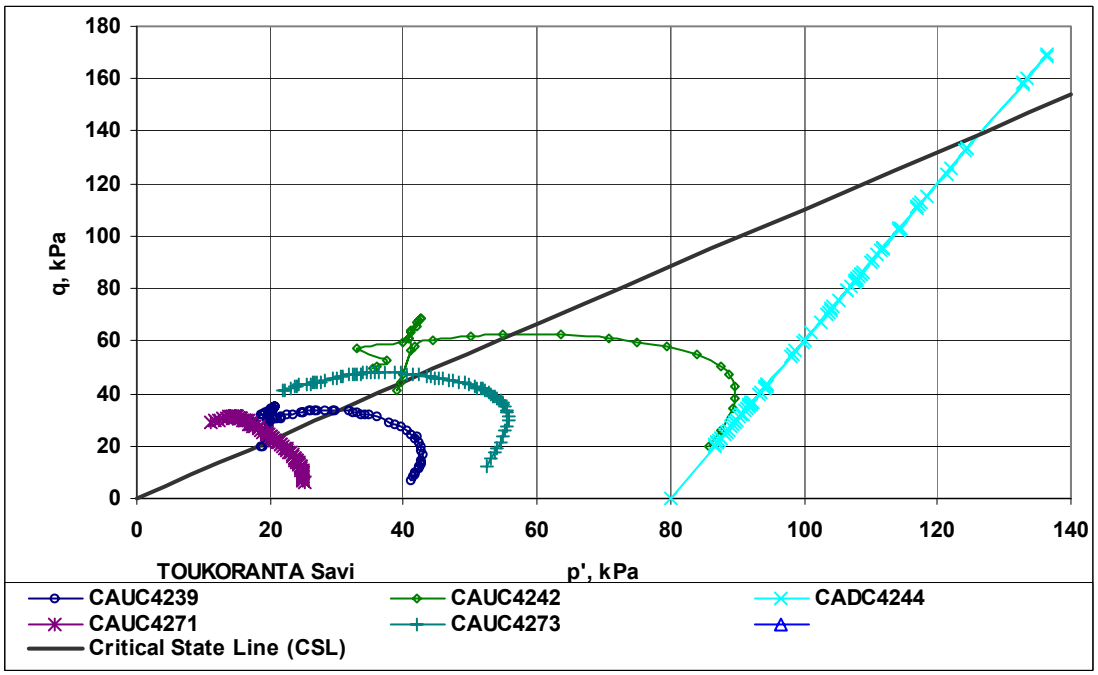

Figure 2.11: *Stress path in triaxial test to determine critical state line*

3. MATERIAL MODEL

In this chapter material model is discussed (PLAXIS V:8). The mechanical behaviour of soils may be modeled at various degrees of accuracy. Hooke's law of linear, isotropic elasticity is the simplest available stress-strain relationship. As it involves only two input parameters, i.e. Young's modulus, *E,* and Poisson's ratio, *v*, it is generally too crude to capture essential features of soil and rock behaviour. For modeling massive structural elements and bedrock layers, however, linear elasticity may be appropriate.

3.1 Mohr-Coulomb model (MC)

In Mohr-Coulomb model shear strength is a function of effective stress, cohesion and angel of internal friction. Coulomb's soil model is expressed in Equation 2.12 and in Fig 2.12. This soil model makes no statement about strains and assume soil doesn't strain harden before failure. For such ideal soil, yield and failure are simultaneous. A material neither hardens nor softens in this way is said as perfect plasticity (Fig 3.1). In order to evaluate whether or not plasticity occurs in a calculation, a yield function *f*, is introduced as a function of stress and strain.

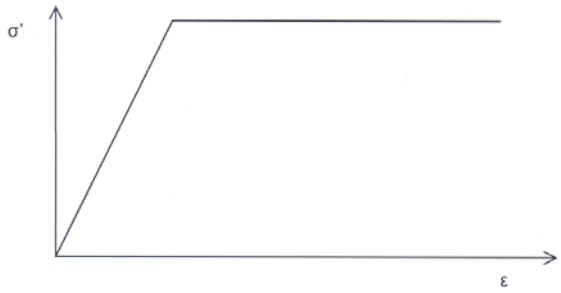

Figure 3.1*: Elastic-perfectly plastic stress-strain relation*

The basic principle of elastoplasticity is that strains and strain rates are decomposed into an elastic part and a plastic part. Hooke's law is used to relate the stress rates to the elastic strain rates (Equation 3.1).

$$\dot{\underline{\varepsilon}} = \dot{\underline{\varepsilon}}^{e} + \dot{\underline{\varepsilon}}^{p} \quad \text{.....(3.1a)}$$

$$\dot{\underline{\sigma}}' = \underline{\underline{D}}^{e}\,\dot{\underline{\varepsilon}}^{e} = \underline{\underline{D}}^{e}(\dot{\underline{\varepsilon}} - \dot{\underline{\varepsilon}}^{p}) \quad \text{.....(3.1b)}$$

where, $\underline{\dot{\varepsilon}}$ is strain rate, $\underline{\dot{\varepsilon}}^{e}$ elastic strain rate, $\underline{\dot{\varepsilon}}^{p}$ Plastic stain rate, $\underline{\dot{\sigma}'}$ effective stress increment, and $\underline{\underline{D}}^{e}$ elastic material matrix.

According to the classical theory of plasticity (Hill, 1950), plastic strain rates are proportional to the derivative of the yield function with respect to the stresses. This means that the plastic strain rates can be represented as vectors perpendicular to the yield surface. This classical form of the theory is referred to as associated plasticity. However, for Mohr-Coulomb type yield functions, the theory of associated plasticity leads to an overprediction of dilatancy. Therefore, in addition to the yield function, a plastic potential function g is introduced. The case $g \neq f$ is denoted as non-associated plasticity. In general, the plastic strain rates are written as:

$$\underline{\dot{\varepsilon}}^{p} = \lambda \frac{\partial g}{\partial \underline{\sigma}} \qquad \text{(3.2)}$$

in which λ is the plastic multiplier. For purely elastic behaviour λ is zero, whereas in the case of plastic behaviour λ is positive.

$\lambda = 0$, for $f < 0$ (Elasticity) (3.3a)

$\lambda > 0$, for $f = 0$ (Plasticity) (3.3b)

Yield function based of Mohr-Coulomb (Fig 2.10) is expressed in terms of principal stresses in Equation 3.4 (tension is positive). The full Mohr-Coulomb yield function consists of six yield functions (PLAXIS 8). These yield functions together represents a hexagonal cone in principal stress space (Fig. 3.2).

$$f = \frac{1}{2}\left(\sigma_1' - \sigma_3'\right) + \frac{1}{2}\left(\sigma_1' + \sigma_3'\right)\sin\varphi - c\cos\varphi \qquad \text{(3.4)}$$

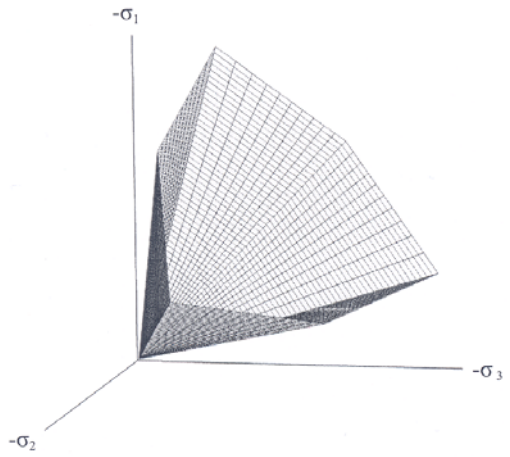

Figure 3.2: *The Mohr-Coulomb yield surface in principal stress space (c = 0 and tension positive in figure)*

The elastic-plastic Mohr-Coulomb model involves five input parameters, i.e. E and v for soil elasticity; φ and c for soil plasticity and ψ as an angle of dilatancy. This Mohr-Coulomb model represents a 'first-order' approximation of soil or rock behaviour. It is recommended to use this model for a first analysis of the problem considered. For each layer a constant average stiffness is estimated. Due to this constant stiffness, computations tend to be relatively fast and a first impression of deformations can be obtained. Besides the five model parameters mentioned above, initial soil conditions play an essential role in most soil deformation problems. Initial horizontal soil stresses have to be generated by selecting proper K_0 values.

3.2 Soft-Soil-Creep model (SSC)

Soft soil is generally found normally consolidated state. The special feature of soft soil is high degree of compressibility. All soils exhibit some creep and primary compression is thus followed by a certain amount of secondary compression. In SSC model creep behaviour is taken into account for normally consolidated clays, silts and peat.

Some basic characteristics of SSC model are given below:

- Stress-dependent stiffness (logarithmic compression behaviour)
- Distinction between primary loading and unloading-reloading
- Secondary (time-dependent) compression

- Pre-consolidation stress
- Failure criteria according to Mohr-Coulomb model

The coefficient of secondary compression can be evaluated from the slope of the time-settlement curve after the excess pore pressure dissipation or primary consolidation (Buisman, 1936) (Fig 2.3). He proposed the following equation

$$\varepsilon = \varepsilon_c - C_B \log\left(\frac{t}{t_c}\right) \text{ for } t > t_c \quad \text{.....(3.5a)}$$

or,

$$\varepsilon = \varepsilon_c - C_B \log\left(\frac{t_c + t'}{t_c}\right) \text{ for } t' > 0,\ t' = t\text{-}t_c \quad \text{.....(3.5b)}$$

where, ε_c is the strain up to the end of consolidation, t the time measured from the beginning of loading, t_c the time to the end of primary consolidation and C_B is a material constant.

Garlanger (1972) proposed a creep equation 3.6 in terms of void ratio and consolidation time τ_c. Equation 3.5 and 3.6 are identical when $\tau_c = t_c$.

$$e = e_c - C_\alpha \log\left(\frac{\tau_c + t'}{\tau_c}\right) \text{ and } C_{\alpha\varepsilon} = \frac{C_\alpha}{1 + e_0}, \text{ for } t' > 0 \quad \text{.....(3.6)}$$

Butterfield (1979) proposed creep effects in terms of natural logarithmic scale.

$$\varepsilon^H = \varepsilon_c^H - C \ln\left(\frac{\tau_c + t'}{\tau_c}\right) \quad \text{.....(3.7)}$$

where, $C = \dfrac{C_\alpha}{(1 + e_0).\ln 10}$, ε^H is logarithmic stain.

To evaluate parameter C and τ_c Janbu (1969) developed the following Equation 3.8. In Equation 3.8 and in Fig 3.3, compressive strain is considered negative. The use of the Janbu method is attractive, because both τ_c, and C follow directly when fitting a straight line through the data. In Janbu's representation of Fig 3.3 b, τ_c, is the intercept with the (non-logarithmic) time axis of the straight creep line. The deviation from a linear relation for $t < t_c$, is due to consolidation.

$$-\dot{\underline{\varepsilon}} = \frac{C}{\tau_c + t'} \quad \text{or, inversely} \quad -\frac{1}{\dot{\underline{\varepsilon}}} = \frac{\tau_c + t'}{C} \qquad \text{.....(3.8)}$$

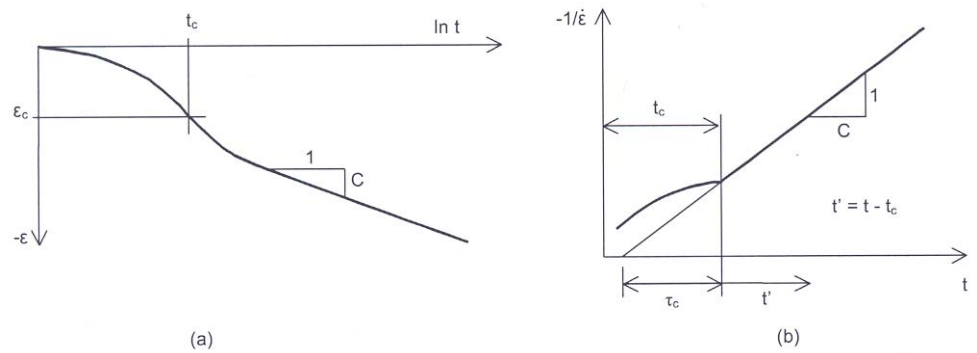

Figure 3.3*: Consolidation and creep behaviour in standard oedometer test (compression negative)*

Therefore strain due to an increase in effective stress from σ_0' to σ' and a time period of t_c+t' is expressed by Equation 3.9.

$$\varepsilon = A\ln\left(\frac{\sigma'}{\sigma'_0}\right) + B\ln\left(\frac{\sigma_{pc}}{\sigma_{p0}}\right) + C\ln\left(\frac{\tau_c + t'}{\tau_c}\right) \qquad \text{.....(3.9)}$$

where

$$A = \frac{C_c}{(1+e_0).\ln 10}, B = \frac{(C_c - C_r)}{(1+e_0).\ln 10}$$

and σ_{p0} and σ_{pc} represent preconsolidation pressure corresponding to before loading and end-of-consolidation states respectively.

4. TOUKORANTA

4.1 General

Toukoranta is situated in the eastern part of Helsinki near the outlet of river Vantaa. The area was considered completely unsuitable for building purposes thereby served mainly as a filling area. As a result of the filling activity almost all of the land area was eventually reclaimed. In the winter of 1985, The City of Helsinki completed the reclamation operation by placing filling material over the frozen sea (Leppänen 1989). The acreage of the grounds covered by the city plan was about 0,85 km^2 and it was planned for approximately 8000 inhabitants as dwelling purposes (Gulin and Wikström 1997).

4.2 Ground profile

In-situ site investigation and laboratory tests were carried out to get soil profile. *In-situ* site investigations were performed by The City of Helsinki on 2004. *In-situ* site investigation results are presented in Fig 4.1. Undisturbed soil samples were collected around the middle of 2004. All the laboratory tests were performed in the Laboratory of Soil Mechanics and Foundation Engineering at Helsinki University of Technology (HUT). The index properties and oedometer test results are presented in Fig 4.2 and in Fig 4.3 respectively. All the oedometer tests data are attached in Appendix 1.

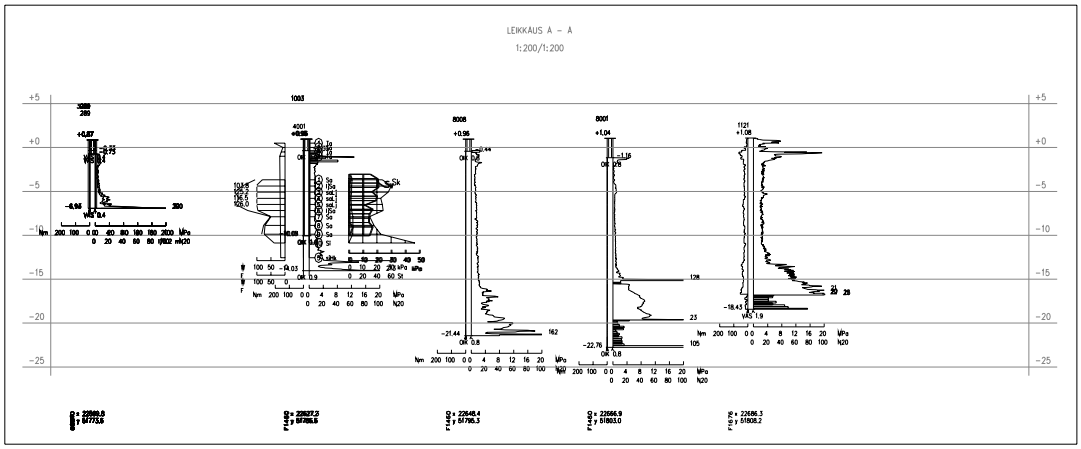

Figure 4.1: *In-situ site investigation of Toukoranta (2004, The City of Helsinki)*

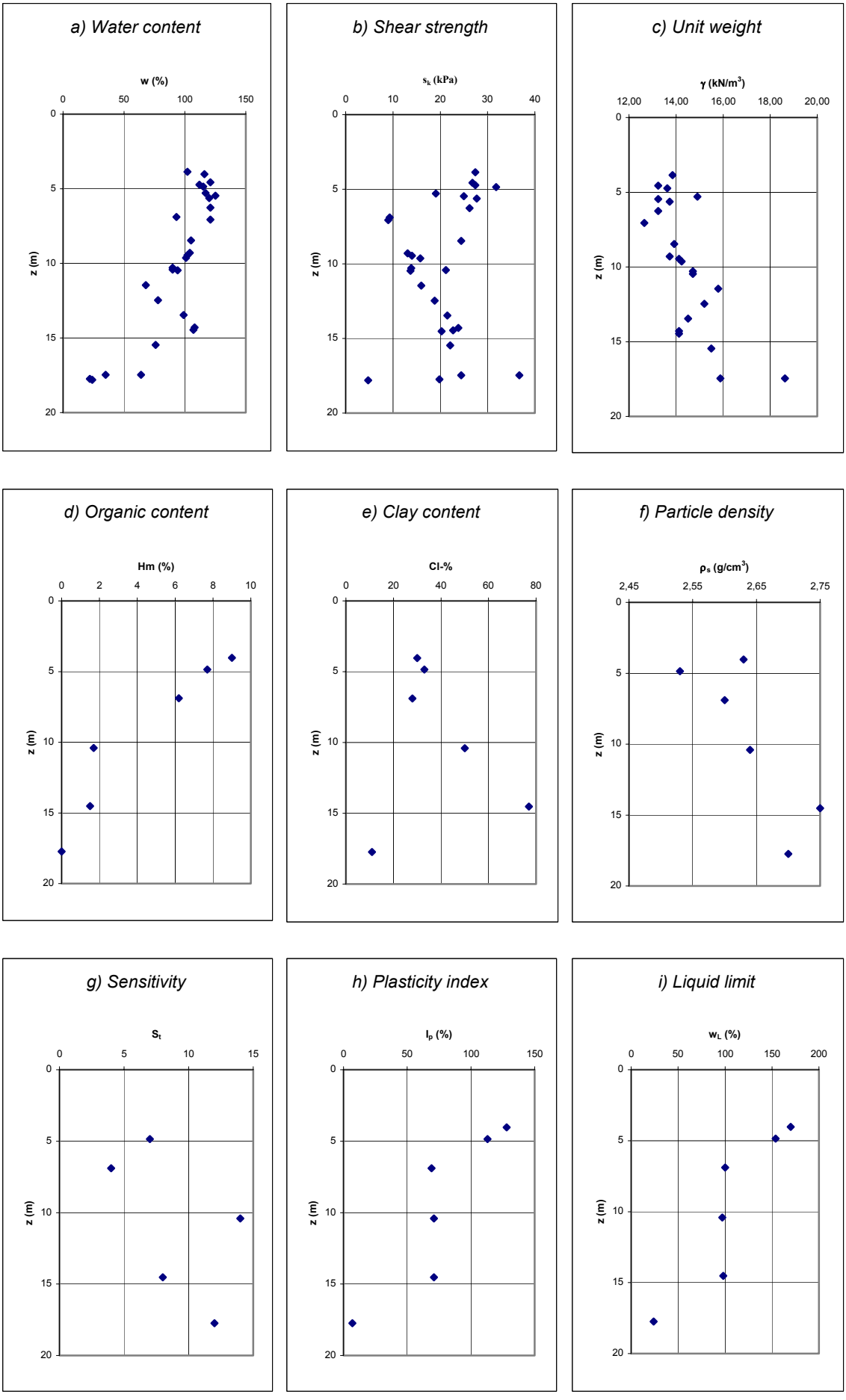

Figure 4.2: *Index properties of (PL 45 St 2) of Toukoranta (2004, HUT)*

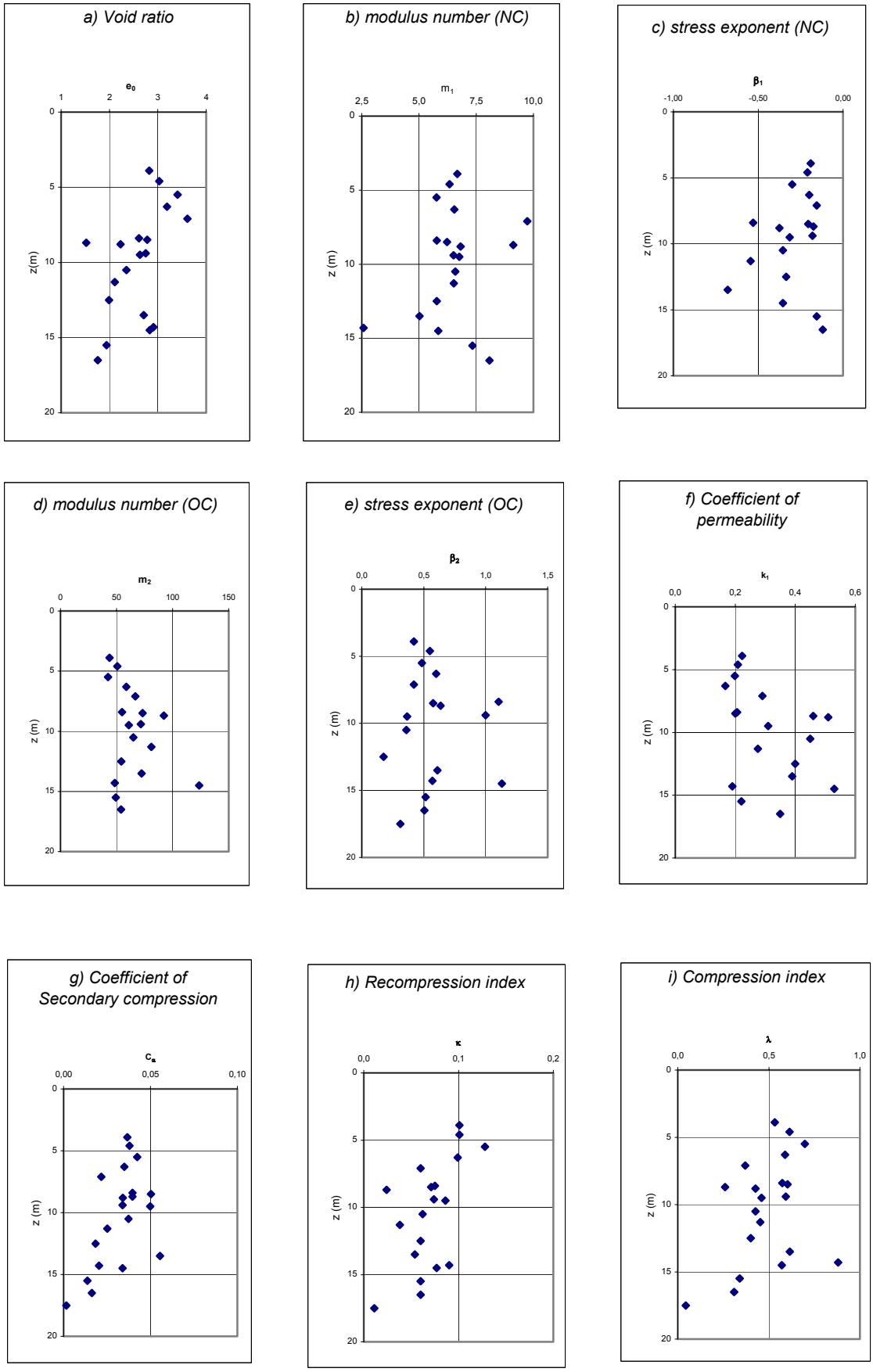

Figure 4.3*: Oedometer test results of Toukoranta, PL 45 St 2, (2004, HUT)*

The deposit is roughly divided into five layers-fill layer, organic clay, clay, silt and sand. The thickness of the soil layers varies from location to location as well as the bottom rock level. The index properties of the site are presented in Figure 4.2. The top fill layer reclamation was started since the late 19th century and after the reclamation operation the finished thickness was about 4 meters. The next soil layer below the fill layer is distinguished as soft organic clay of a thickness approximately 8 meters. 'The organic layer was deposited some 8,000 years ago into the Lithorina Sea (Gulin and Wikström 1997)'. The natural water content of the organic clay layer varies between 100 to 130 percent and has 6 to 9 percent organic content. Liquid limit (w_L) of this layer is more than 150 percent and plasticity index I_p is more than 100 percent. Below the organic clay layer, there is another clay layer that is also about 8 meter thick and has natural water content between 70 to 100 percent. Near the bottom, occasional silt and sand layers are found. The bottom layer is bedrock and considered as free draining layer.

In Finland, Janbu's (1963) tangent modulus method is commonly used for settlement calculations. The parameters, modulus number m and stress exponent β can be determined from oedometer test results. Modulus number m_1 (NC) varies between 5 to 7.5 and stress exponent β_1 (NC) lies between 0 to –0.5. Void ratio of the soft organic layer varies between 3 to 4 and the clay layer has void ratio between 2 to 3.
The deposit is found in normally consolidated state.

4.3 History of reclamation and test construction

The top fill layer reclamation was started on the site around 1963 and lasted about 10 years. The original ground level was below sea more than 1 meter. The City of Helsinki fully reclaimed the area in 1985 and the finished formation level was more than +1 meter.

In order to obtain information from design, construction, and deformation point of view The City of Helsinki constructed a test embankment with an adjacent excavation in 1995. A plan view of the test embankment and excavation is presented in Fig 4.4.

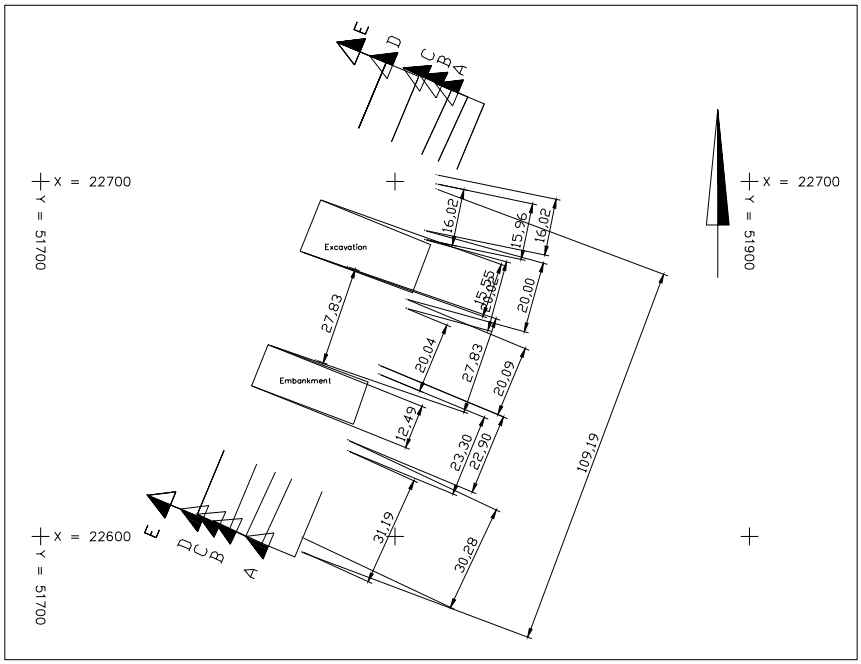

Figure 4.4*: Plan view of the test embankment and excavation (1996, The City of Helsinki / Fundus)*

The base dimension of the embankment and excavation were 12,5 x 35 m^2 and 15 x 35 m^2 respectively. The distance between the embankment and the excavation was 27 meters. Both the embankment and the excavation were completed in two stages. The first stage construction of the excavation and the embankment began approximately on the first week of October 1995 and completed within 7 days. After the first stage of operation the embankment was 1.4 m high and the excavation reached 1.1 m deep having 1:1 slope. The first stage operation lasted for more than one and half month. The second stage of the operation was started on the middle of November 1995. This operation took approximately 10 days. After the final stage of operation, width and height of the top of the test embankment were 8.7 m and 1.9 m respectively and the excavation width and depth were 11.6 m and 1.7 m respectively. Both the

embankment and the excavation construction had 1:1 slope. Inclinometers were installed around the embankment and the excavation and horizontal deformation measurement was started from 20th Novmeber 1995 (Gulin and Wikström 1997) and continued up to February 1996. Cross-sectional view of the completed embankment and excavation and inclinometer positions are presented in Fig 4.5.

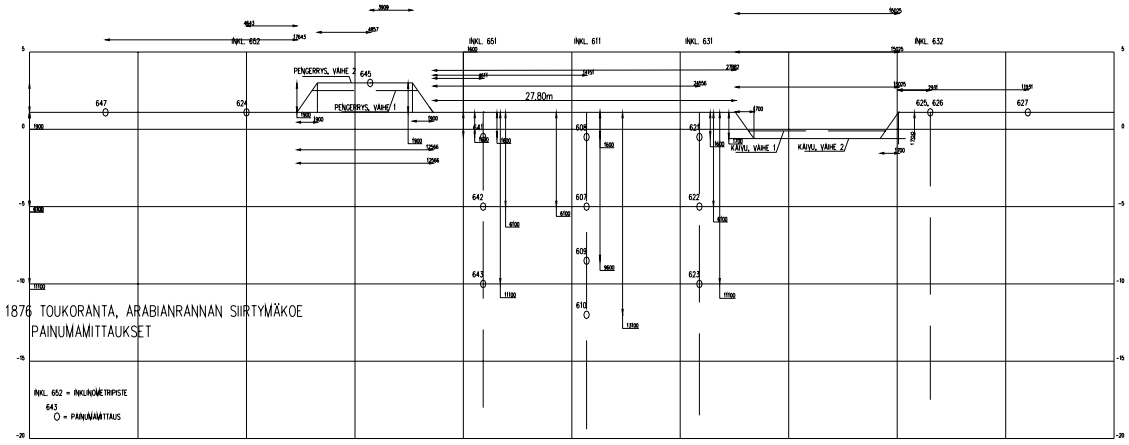

Figure 4.5: *Cross-sectional profile of the test embankment and excavation (1996, Fundus)*

4.4 Finite element calculation

4.4.1 Initial information

Geometry of the area, geological profile, and geometry of the embankment and the excavation used in FEM calculation are presented in Fig 4.6. Soil layers and bottom rock level varies in thickness from location to location. Bottom rock level forms a small valley type formation and both on the edges its thickness is much higher than the apparent center of the studied area. Soil deposit is thickest at the apparent center of the area.

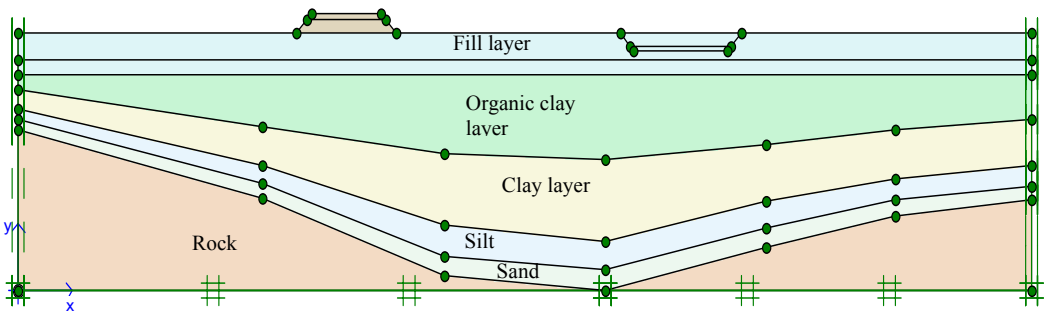

Figure 4.6: *Geometry and the geological profile of Toukoranta (1996) used in FEM calculation*

The top fill layer and the test embankment have been modelled with Mohr-Coulomb material (MC model). The organic clay layer, clay layer, and silt layer below the filling layer have been modelled with Soft Soil Creep (SSC) model. The failure and yield surfaces of Soft-Soil Creep model are presented in Fig 4.7: the failure surface is formed according to the Mohr-Coulomb failure criteria and the yield surface (cap) according to modified Cam Clay model that includes cohesion.

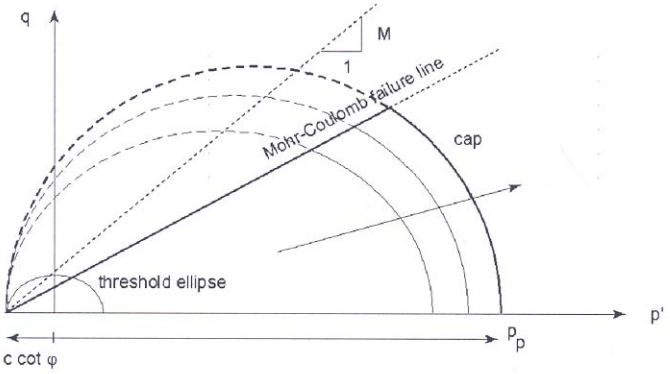

Figure 4.7: *The failure and yield surface of SSC model: the mean effective p' and deviator stress q. M is the slope of the critical line. (compression positive in Figure)*

The layers and their parameters are presented in Tables 4.1 to 4.4. Parameters given for SSC model have been evaluated from laboratory tests in 2004. MC model parameters are approximated values.

Table 4.1: *The layers and overconsolidation conditions used in PLAXIS*

Layer number	Soil Type	Thickness, (approx. at the middle) m	Material Model	POP, kPa
1	Fill layer	4	MC	Not used
2	Organic Clay layer	8,4	SSC	0
3	Clay layer	8	SSC	0
4	Silt	2,8	SSC	0
5	Sand	2	MC	Not used
6	Embankment	-	MC	Not used

Table 4.2: *Parameters of Soft Soil Creep model part 1*

Layer number	γ_{dry} kN/m^3	γ_{wet} kN/m^3	k_x m/day	k_y m/day	C_k	λ^*	κ^*	μ^*
2	3,0	13,0	3,456E-5	3,456E-5	1,0	0,197	0,015	0,024
3	13,5	14,5	5,184E-6	5,184E-6	1,0	0,221	0,02	0,013
4	17,5	18,5	8,64E-5	8,64E-5	1,0	0,045	0,0064	0,0095

Table 4.3*: Parameters of Soft Soil Creep model part 2*

Layer number	ν_{ur}	K_0^{nc}	c' kN/m^2	ϕ'°	ψ°	e_{init}
2	0,15	0,694	2,0	27,7	0	3,429
3	0,15	0,694	2,0	27,7	0	2,451
4	0,15	0,692	2,0	27,7	0	0,902

Table 4.4: *Parameter of Mohr-Coulomb model*

Layer number	γ_{dry} kN/m^3	γ_{wet} kN/m^3	k_x m/day	k_y m/day	ν	E kN/m^2	c' kN/m^2	ϕ'°	ψ°
1	14,0	16,0	1,0	1,0	0,35	3,0E+4	10,0	30	0
5	16,0	18,0	5,0	5,0	0,35	3,0E+4	1,0	30	0
Embankment	16,0	18,0	1,0	1,0	0,35	4,0E+4	1,0	34	0

Parameters presented in previous tables (PLAXIS manual, version 8.2):

γ_{dry} Total unit weight of soil above groundwater level, kN/m^3

γ_{wet} Total unit weight of soil below groundwater level, kN/m^3

λ^* Modified compression index (NC)

κ^* Modified swelling index (OC)

μ^* Modified coefficient of secondary compression

k_x Coefficient of horizontal permeability in initial state (=k_{0x})

k_y Coefficient of vertical permeability in initial state (=k_{0y})

ν,ν_{ur} Poisson's ratio, Poisson's ratio (unloading-reloading)

e_{init} Initial void ratio

C_k Factor of change permeability

The overconsolidation conditions are characterised with parameter POP in Equation (4.4.1).

$$POP = \left(\sigma_c - \sigma_{yy}^0\right) \geq 0 \quad \text{.....(4.4.1)}$$

where, σ_c is the consolidation stress and σ_{yy}^0 the current effective vertical stress.

The decrease of the permeability is considered as presented in Equation (4.4.2)

$$\lg\left(\frac{k}{k_0}\right) = \frac{\Delta e}{C_k} \quad \text{.....(4.4.2)}$$

where k is the changed coefficient of permeability and Δe is the change in void ratio during consolidation.

15 node triangular elements have been used in calculation. Plane strain conditions have considered for calculation. The finite element mesh (Appendix 2.1) has a width 126 m and covered the soil condition down to the bedrock. The lateral boundaries have been fixed in horizontal direction and the bottom boundary has taken as fixed in the horizontal and vertical direction. The boundary conditions of consolidation have been open at the ground surface, on the bottom of the mesh during the consolidation stage (Appendix 2.1).

Modelling order used for calculation is presented below:

1. Calculation of the initial stresses
2. Adding the load by the filling material, 1985
3. Back calculation 10 years of consolidation, 1985-1995
4. Adding the first stage construction and excavation, October 1995
5. Consolidation of the next 44 days
6. Adding the second stage of construction and excavation, November 1995
7. Consolidation of the next 90 days, February 1996

4.5 Results and discussion

In this section finite element calculation results are presented.

Filling operation was started a long time before 1985. The area was fully reclaimed from sea in 1985 by placing filling material over frozen ice. In FEM calculation, it has been assumed that the reclamation of the whole area is done in a single operation to simplify the calculation. In this plastic calculation phase silt layer and clay layers have been assumed undrained. In Appendix 2.2a, the distribution of excess pore pressures just after the reclamation is presented. Maximum excess pore pressures generate inside the silt layer (layer 4) around the apparent center of the area and excess pore pressure varies from 98 to 60 kPa in this layer. Excess pore pressure varies from 45 to

75 kPa inside the organic clay layer (layer 2) and the clay layer (layer 3). It can be concluded that, excess pore pressure generation in this calculation phase is only coarse approximation because of the simplification of the actual events and in reality field excess pore pressure would be lower.

Excess pore pressures, vertical and horizontal displacements 10 years after reclamation or consolidation are presented in Appendix 2.3. 10 years of consolidation allows full dissipation of excess pore pressure from the silt layer (layer 4). Because of low coefficient of permeability and long drainage path, dissipation of excess pore pressures of the clay layers is small. The excess pore pressures of the clay layers corresponding to this moment vary between 40 to 67 kPa. This back analysis reveals that a little increment in effective stress would have occurred in large parts of the clay deposit.

The calculated maximum vertical settlement corresponding to this moment is approximately 1130 mm. Vertical settlements are approximately uniform and more than 1000 mm of the whole area (Appendix 2.3b). The clay layers mainly contributed these settlements. The calculated time-settlement behaviour of point A (54.95, 25.2) is presented in Fig 4.8.

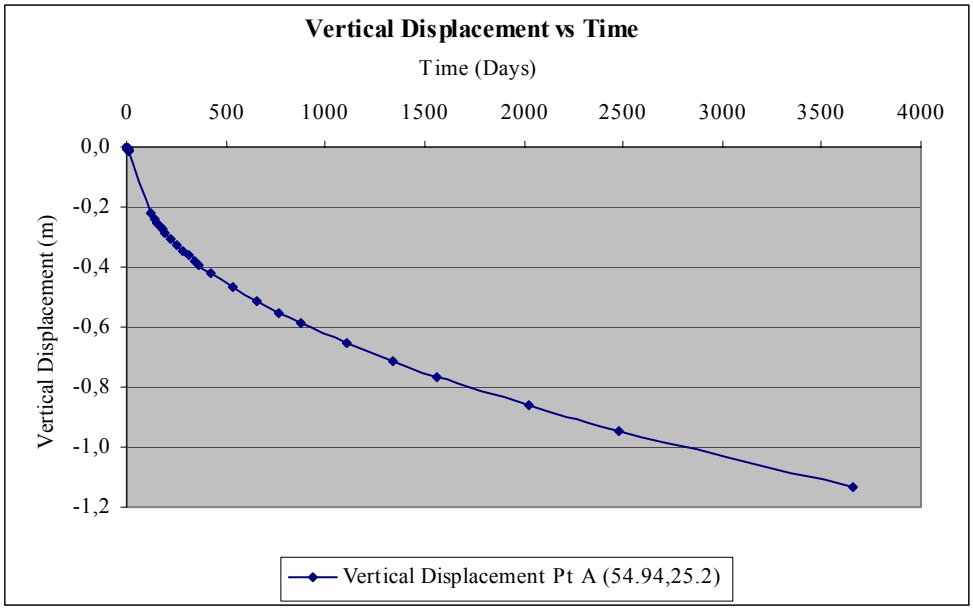

Figure 4.8: *Calculated vertical settlement of 10 years (1985-1995)*

The consolidation process is accompanied with horizontal deformation. Horizontal deformation 10 years after reclamation is presented in Appendix 2.3c. Maximum

horizontal displacement corresponding to this moment is 31 mm and clay layers (layer 2 and layer 3) shows tendency to move towards to the apparent center. External factors like fluctuation of ground water table, varying water contents of the deposit, temperature variation, snow and freezing affect different layer differently and sometimes work in opposite direction, there is no simple way to take account of them.

First stage operation of the test embankment and excavation was completed on the first week of October 1995. In Appendix 2.4, excess pore pressure, vertical and horizontal displacement of this phase are presented. Adding stresses by the embankment and also unloading by the excavation influence the pore pressures generation of soil deposit. Maximum pore pressure generates inside the clay layers just below the embankment and varies between 40 to 70 kPa. Unloading because of the excavation influences excess pore pressures to drop. Horizontal and vertical deformations after the first stage of operation are small (Appendix 2.4b, 2.4c). Vertical settlements occur below the embankment and maximum vertical settlement corresponding to these moments is approximately 45 mm. Unloading by excavation induce swelling around the excavated area. Maximum heave corresponding to this moment is 38 mm. Horizontal displacements show some mixed behaviour because of changed stress distribution after construction. Clay deposit of at center of the area, horizontally displace positively. Maximum horizontal deformation is approximately 36 mm, mainly concentrated in the organic clay layer.

The first stage construction lasted approximately more than one and half month. In FEM calculation it has taken approximately 44 days. Consolidation effects for this small time span are presented in Appendix 2.5. Excess pore pressures dissipation is very small and extreme excess pore pressures corresponding to this moment approximately is about 70 kPa. Maximum vertical displacements are 80 mm below the embankment and maximum horizontal displacements are 52 mm.

The last stage of construction operation was started at the end of November 1995. The test embankment was raised by 0.5 m and excavation was also reached its final depth by cutting extra 0.5 m of fill material. This operation was completed within 7 days. This small loading and unloading influenced little of the whole soil profile. Excess pore pressures, horizontal, and vertical displacements are presented in Appendix 2.6. Extreme excess pore pressures increase from 70 kPa to 72 kPa inside the clay layers

below the embankment. Below the excavation excess pore pressures decrease small. Extreme horizontal displacements and vertical displacements are 69 mm and 102 mm respectively.

The last stage of operation was allowed to continue up to February 1996. After measuring the horizontal displacements the test embankment was removed and the test excavation was filled up. The consolidation results of this 90 days time frame are presented in Appendix 2.7. Excess pore pressure dissipation is small of the soil deposit. Inside the clay layers bottom of the test embankment, excess pore pressure increased approximately by 0.65 kPa, this unusual phenomenon may be because of the extra pressure exerted by the inclined downward movements of the clay layers along the bottom rock level and settlement (Appendix 2.7d) Extreme vertical and horizontal settlements corresponding to this moment are 169 mm and 107 mm respectively.

In Appendix 2.7e, some points have selected to study displacements with time. The co-ordinates of the points are given in Table 4.5 below:

Table 4.5: *Coordinates of the selected points*

Point number	Depth (m)	X-coordinate	Y-coordinate
A	0	54,94	25,20
B	4	54,87	21,20
C	7,79	56,03	17,41
D	11,81	56,00	13,39
E	15,3	56,30	9,90

In Fig 4.9, calculated horizontal displacements with time are presented. Starting time 3660 days and horizontal displacements zero represents the beginning of the study October, 1995. The end time 3820 days refers February 1996 or the end of the test.
Pt. C, which is located at the middle of the organic clay layers and approximately 9 m from the toe of the embankment and horizontally displaced 93 mm. From other points, Pt. B, which is located on top of the organic clay layer horizontally, displace approximately 70 mm.

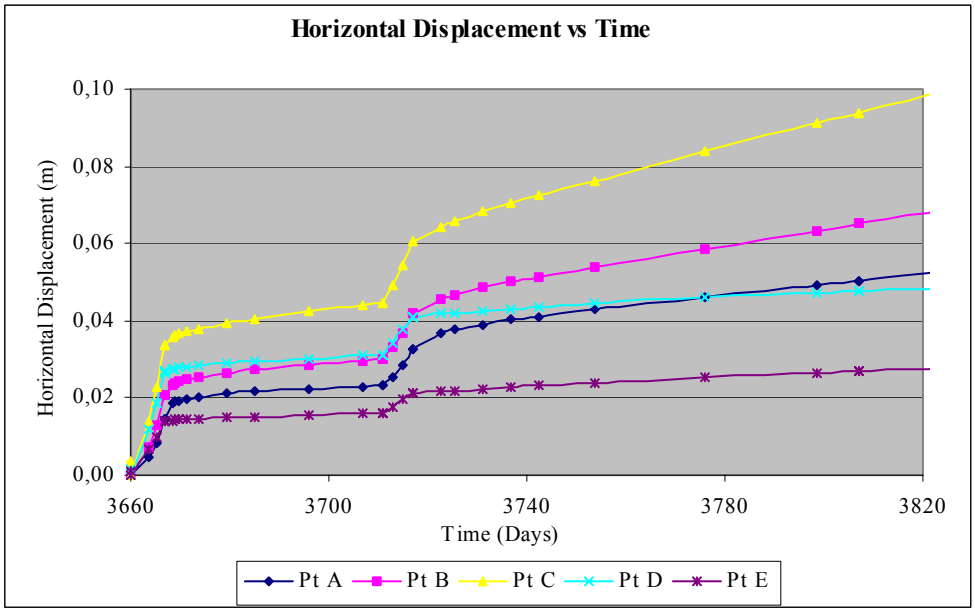

Figure 4.9: *Calculated horizontal displacements with time (October, 1995 – February, 1996)*

The observed horizontal displacements up to 20th February 1996 are presented in Fig 4.10 (Gulin and Wikström 1997). Calculated horizontal displacements of the inclinometers, corresponding time February 1996, versus depth are presented in Fig 4.10 (Appendix 2.7c). It can be concluded that observed and calculated maximum horizontal displacements are fairly close. Calculated maximum horizontal displacement of inclinometer 651 in the middle of the organic clay layer is 101 mm and observed result was approximately 93 mm. Observed maximum horizontal displacements of inclinometer 631 was 75 mm and calculated one is approximately 79 mm. Discrepancy found between the calculated and observed horizontal displacements at the fill layer. Inclinometer 652 showed approximately -26 mm displacement at the formation ground level, contrary calculated displacements is 13 mm. Also calculated and observed horizontal displacements of other inclinometers on the top of the formation ground level are not fairly close. This may be because of the difference in material properties of the fill materials from location to location and also complex stress distribution and imposed boundary condition on modelling.

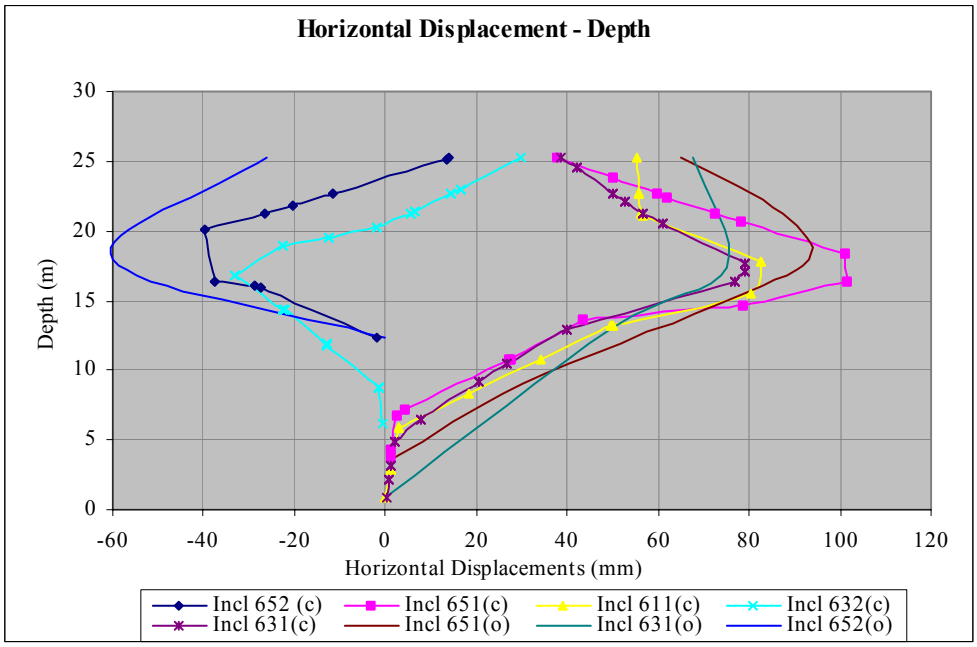

Figure 4.10: *Calculated(c) and observed(o) horizontal displacement- depth (February, 1996)*

Despite the close agreement between the calculated and the observed horizontal displacements for that small time frame, long term observation of pore pressures, settlement distribution, and horizontal displacements are needed to validate the FEM calculation. In reality, the following phenomenons have strong influence on stability, deformation and time-settlement behaviour, but in FEM calculation it is hard and sometimes impossible to take account of them.

- The parameters used in the calculation are evaluated based on small-scale specimen testing. The problem is that small specimens are not always representative for the soil mass.
- The intensity of the applied load by the fill and the embankment is not always certain. This uncertainty may affect the load intensity in the field situation.
- The sequence of load application of embankment and unloading of excavation is a coarse approximation of the exact construction schedule.
- Disturbance during construction is also one of the concerns and may cause uneven stress distribution. According to Gulin and Wikström (1997) 'Due to the technique used in construction of embankment in the area, the land fill was penetrated unevenly into the soft organic clay layer and led to a variation in the stresses in the clay layers'.

- The groundwater level is assumed constant through out the whole simulation, but groundwater table fluctuates from season to season. Other geological factors and also changes in temperature and seasonal snow affect the field condition.
- Groundwater level is assumed to be stationary and associated load reduction due to settlements is not taken into account.

5. HORIZONTAL PERMEABILITY

5.1 General

The consolidation settlement of soft clay creates a lot of problems in foundation and infrastructure engineering. Because of the very low clay permeability, the primary consolidation takes a long time to complete. To shorten consolidation time, vertical drains can be used together with preloading by surcharge embankment or vacuum pressure. Vertical drains are artificially created drainage paths, which can reduce the consolidation time by shortening the drainage path and using horizontal flow. Most natural soft-clay deposits are more-or-less anisotropic with respect to their flow properties. Typically, the horizontal permeability or flow is higher than that for flow in the vertical direction. Therefore, when horizontal flow predominates, vertical drains generally give an additional benefit to time-settlement behaviour.

5.2 Measurement of coefficient of horizontal permeability

Coefficient of horizontal permeability can be measured directly or indirectly in controlled environment in laboratory or *in-situ*. Direct measurement of coefficient of horizontal permeability is always better than indirect evaluation. In view of the limitations of laboratory tests, permeability characteristics can be obtained from appropriate *in-situ* testing. This report focuses on the laboratory determination of coefficient of horizontal permeability k_h.

The usual approach for the determination of horizontal permeability characteristics in the laboratory is from ordinary oedometer tests. A better approach is to determine c_h or k_h in oedometer tests in which radial drainage is allowed. Rowe cells can be modified to determine horizontal permability. To avoid uncertainties associated with the natural variability of clays on the evaluation of permeability anisotropy, it is preferable to measure the vertical and horizontal permeability on the same specimen. Chan and Kenney (1973) developed such a technique in which a cubic specimen was rotated 90° to measure permeability in both directions. Drawback of this technique is that it cannot readily be used to measure vertical and horizontal permeability at different void ratios.

5.2.1 Vertical cut sample

Coefficient of horizontal permeability k_h can be determined using vertical cut sample from undisturbed sample and can be tested in the usual manner. Evaluation of the time-settlement parameters are same. From time-settlement curve, time for 50 % and 90 % can be evaluated by using Casagrande's or Taylor's method, presented in Section 2.1.4. The coefficient of consolidation c_h of horizontal flow can be obtained using Equation 2.7 and Equation 2.8.

Direct determination of coefficient of permeability k can also be performed using modified oedometer for clay suggested by Tavenas *et. al*. (1983b). This procedure follows falling head permeability test method and the Equation 2.11 (presented in 2.1.6) is used to determine coefficient of permeability. It can be argued that the strain or compression occurs in wrong direction. The basic assumption is that horizontal flow is independent to the direction of stress and compression (Leminen and Rathmayer 1983).

Leminen and Rathmayer, in 1983, presented their experience on horizontal oedometer tests to determine coefficient of consolidation for horizontal flow c_h. They argued that the assumption of horizontal flow is independent to compression, and no significant errors would occur as long as the inner structure suffers no essential disturbance. Fig 5.1 shows a schematic diagram of vertical cut sample and Equations to evaluate consolidation parameter.

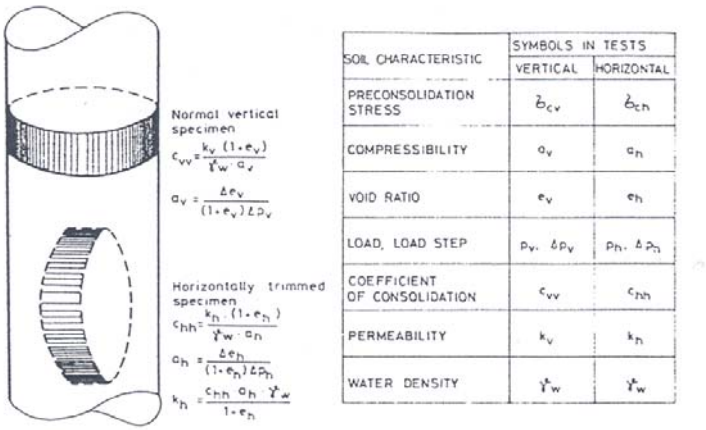

SOIL CHARACTERISTIC	SYMBOLS IN TESTS	
	VERTICAL	HORIZONTAL
PRECONSOLIDATION STRESS	σ_{cv}	σ_{ch}
COMPRESSIBILITY	a_v	a_h
VOID RATIO	e_v	e_h
LOAD, LOAD STEP	p_v, Δp_v	p_h, Δp_h
COEFFICIENT OF CONSOLIDATION	c_{vv}	c_{hh}
PERMEABILITY	k_v	k_h
WATER DENSITY	γ_w	γ_w

Figure 5.1: *Schematic diagram of vertical cut sample testing (Leminen and Rathmayer 1983)*

5.2.2 Radial-flow permeameter

To measure the coefficient of horizontal permeability directly, 'Radial-flow permeameter') was used by Leroueil *et.al.*(1990). A schematic figure of that 'Radial-flow permeameter' is presented in Fig 5.2. The cell ring diameter of that permeameter was 180 mm and height 90 mm. The central injection hole was 50 mm and samples were compressed between two rigid and parallel platens, so that flow of water was forced horizontally from the central injection hole to the circumferential drain.

The central drain was made of geotextile with high permability ($k \approx 10^{-5}$ m/s) and high compressibility. The reduction in diameter of geotextile drain was found only 3% after vertical compression of the specimen up to 25-30%. The lateral circumferential drain was a thin, cylindrical plate of porous stainless steel that was inserted, but not fixed, within a rigid oedometer ring. The permeability of that material was high (($k \approx 10^{-5}$ m/s). To avoid any smearing precaution was taken while placing the sample. That permeameter was placed in cell 300 mm in diameter and 200 mm high to introduce back pressure. A constant strain rate (about 2% per day) was applied up to the desired strain and excess pore pressure was allowed to dissipated. However load reduction was approximately 20% during this equilibrium-testing phase. Constant head permeability were performed with an 'average gradient' of about 10, where water-pressure difference was 6.4 kPa between central drain to outer drain Eq. 5.1.

$$i = \frac{h}{l} = \frac{2\Delta u}{\gamma_w \left(d_e - d_i\right)} \qquad \text{.....(5.1)}$$

where, i is average hydraulic gradient

Δu water pressure difference

d_e external diameter of the specimen

d_i diameter of drain/intial diameter of sample

The volume of the water flowing from the central hole to outer drain was measured. The coefficient of horizontal permeability was measured by Equation (5.2).

$$k_h = \frac{Q}{2\pi H \Delta h} \cdot \ln\left(\frac{r_e}{r_i}\right) \qquad \text{.....(5.2)}$$

where , Q is the flow rate

r_e and r_i are the external and internal radius

Δh is the water head difference between the central injection hole to outer drain

H is the height of the sample

However, the authors argued that the friction between the sample and the central drain was 'unknown', though water content profile after testing of the sample didn't show significant friction effect between circumferential drain and soil.

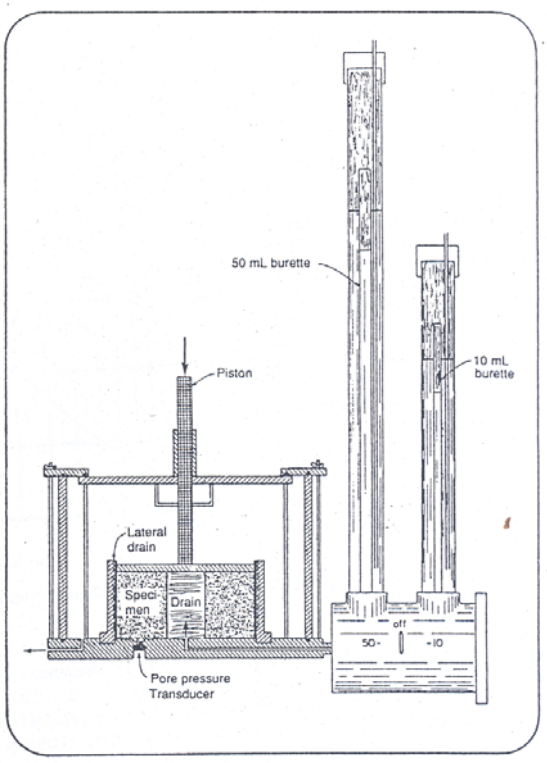

Figure 5.2: *Radial flow permeameter (Leroueil et.al.1990).*

5.2 Consolidation theories based of horizontal flow

5.2.1 Barron's method

Barron in 1948 presented his consolidation theory based on vertical drain or horizontal flow. His theory was based on the simplifying assumptions of Terzaghi's one-dimensional theory. Barron (1948) also addressed the boundary condition both on the equal and free strain condition based on pure horizontal flow. However, comparison between Barrons's (1948) free and equal strain theory solutions indicates

that both yield the same average degree of consolidation when drain spacing ratio (n) is greater than 5 and time factor (T_h) >0.1. (*cited in* Holtz *et.al*.1991).

In the case of equal strain, the differential equation governing process is given by Eq (5.3):

$$\frac{\partial u}{\partial t} = c_h\left(\frac{\partial^2 u}{\partial r^2} + \frac{1}{r}\frac{\partial u}{\partial r}\right) \quad \text{.....(5.3)}$$

For the case of pure radial drainage, the solution under ideal condition (no smear or no well resistance) is expressed by the Equations 5.4 and 5.5.

$$\overline{U}_h = 1 - \exp\left[\frac{-8T_h}{F(n)}\right] \quad \text{.....(5.4)}$$

where, $\overline{U}_h$ = average degree of consolidation

T_h = time factor = $T_h = \dfrac{c_h t}{D_e^2}$

c_h = coefficient of consolidation of horizontal pore water flow

D_e = equivalent sample diameter

$$F(n) = \frac{n^2}{n^2 - 1} \cdot \ln(n) - \frac{3n^2 - 1}{4n^2} \quad \text{.....(5.5)}$$

where n is the drain spacing ratio

$$n = \frac{D_e}{d_w}$$

5.2.2 Hansbo's method

Hansbo (1981) presented the analysis of consolidation by vertical drains, taking account a zone of smear with reduced permeability and well resistance. The theory of consolidation with vertical drains assumes an equivalent cross-sectional area. Also the solution is greatly simplified assuming the horizontal section remains horizontal throughout the consolidation process (equal strain theory).

Hansbo's analysis of the influence of vertical drainage is based on the following assumptions:

- equal strain theory is valid, irrespective of the radial distance from the drain center
- soil is water saturated
- the drain is circular-cylindrical with diameter *d*,
- the drain has limited discharge capacity
- the installation of a drain causes a circular-cylindrical zone of smear around the drain d_s and lower permeability than in the undisturbed soil
- Darcy's law is valid, *i.e.* the rate of flow is directly proportional to the hydraulic gradient
- the effect of pore water flow in the vertical direction between the drains is neglected
- the total stress is the sum of the effective stresses and the pore water pressure

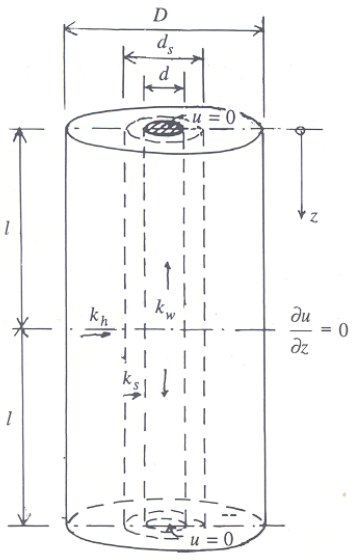

Figure 5.2: *Schematic diagram of vertical drain analysis (Hansbo, 1981)*

These assumption leads to the following approximate solution of the consolidation process (Equation 5.6):

$$\overline{U_h} = 1 - \exp\left[\frac{-8T_h}{F}\right] \quad \text{.....(5.6)}$$

where,

$\overline{U_h}$ = average degree of consolidation

T_h = time factor = $T_h = \dfrac{c_h t}{D_e^2}$

c_h = coefficient of consolidation in horizontal pore water flow

D_e = equivalent drain diameter

$$F = F(n) + Fs + Fr \quad \text{.....(5.7)}$$

and F is the factor which express the additive effect due to drain spacing $F(n)$, smear effect F_s, and well resistance F_r.

The spacing ratio factor simplifies to the following equation 5.8:

$$F(n) = \ln\left[\frac{D_e}{d_w}\right] - \frac{3}{4} \quad \text{.....(5.8)}$$

To account for the effects of soil disturbance during installation, a zone disturbed with a reduced permeability is assumed around the vicinity of the drain, as shown in Fig 5.3. The smear effect is given by the Equation 5.9:

$$F_s = \left[\left(\frac{k_h}{k_s}\right) - 1\right] * \ln\left(\frac{d_s}{d_w}\right) \quad \text{.....(5.9)}$$

where, d_s is the diameter of the disturbed zone around the drain, k_s is the coefficient of permeability in the horizontal direction in the disturbed zone.

Limited discharge capacity of drain is expressed as the well resistance factor F_r, Eq (5.10):

$$F_r = \pi z(L - z)\frac{k_h}{q_w} \quad \text{.....(5.10)}$$

where, z is the distance from the drainage end of the drain, L is twice the length of the drain when discharge occurs at one end only or L is equal to the length of the drain when drainage occurs at both ends, k_h is the coefficient of permeability in the horizontal direction of the undisturbed soil, and q_w is the discharge capacity of the drain at hydraulic gradient of 1.

In general Hansbo proposed the ready computational equation for soil consisting vertical drains that the factor F is expressed by the following equation (5.11):

$$F = \ln\left(\frac{D_e}{d_s}\right) + \frac{k_h}{k_s}\ln\left(\frac{d_s}{d_w}\right) - \frac{3}{4} + \pi(L-z)\left(\frac{k_h}{q_w}\right) \quad \text{.....(5.11)}$$

5.3 Vertical drain (VD) oedometer

To determine horizontal permeability characteristics one oedometer with vertical drain has been developed in the Laboratory of Soil Mechanics and Foundation Engineering, Helsinki University of Technology. The figure of the VD oedometer is presented in Fig 5.4. This is a fixed ring oedometer with inner diameter (D_e) 80 mm. The central drain has a diameter (d_w) of 10 mm and thus drain spacing ratio is (n = D_e/d_w) is 8. Height of the ring is 48 mm and sample height of about 43 mm can be tested. The bottom of the oedometer ring is fixed and has a porous stone. To hinder vertical water flow, insulation is placed on top of the porous stone. That insulation also has a central hole to connect vertical drain to the porous stone. Vertical drain is connected to burette. Water level of burette has been maintained with the same height of the sample and no backpressures develop when water is expelled out from the sample.

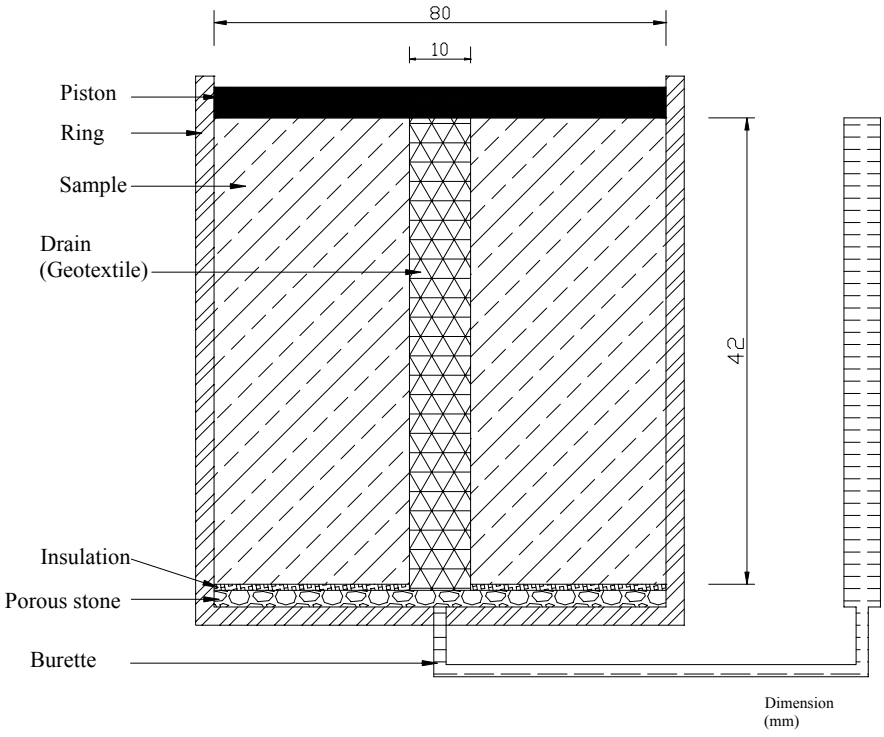

Figure 5.4: *Schematic diagram of vertical drain(VD) oedometer*

The central drain is made of geotextile discs, which are 10 mm in diameter. Falling head permeability test has been performed to check permeability of the used geotextile. Coefficient of permeability of the used textile varies from $3.7*10^{-5}$ to $2.5*10^{-5}$ m/s for relative compression 1.96 % to 28.33 % respectively (Fig 5.5). The geotextile drain shows high permeability and high compressibility. Lateral rigidity of the drain was one of the concerns, but after some preliminary testing it was found the reduction in diameter of geotextile drain was about 2 % to 5 %.

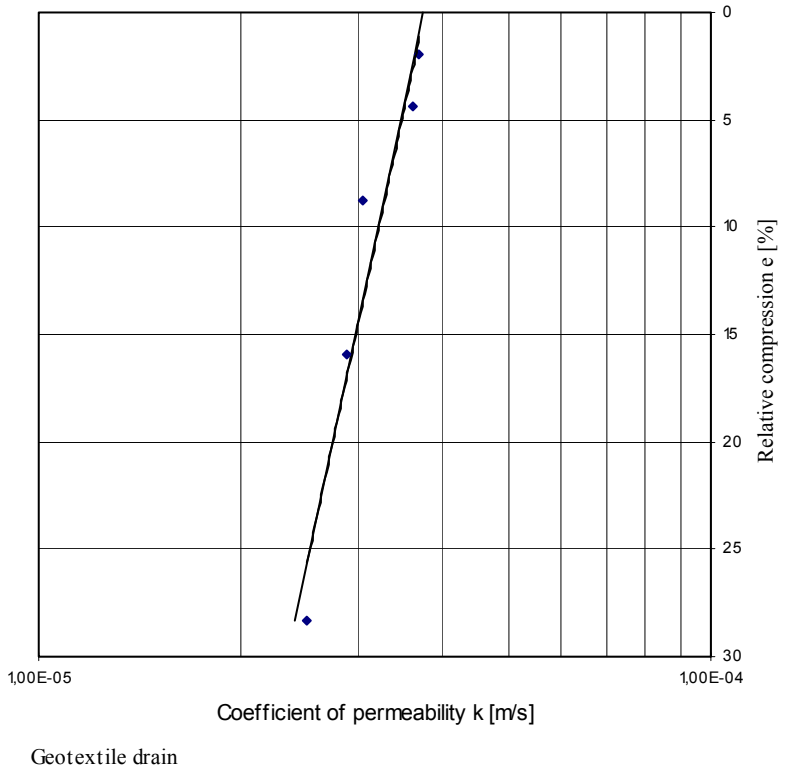

Figure 5.5: *Permeability-relative compression of geotextile drain*

Incremental loading sequence has been used and after 24 hours double stresses have been introduced. Time-settlement has been recorded for every load step to evaluate coefficient of consolidation for horizontal flow.

To avoid smearing care has been taken, though it cannot be claimed that smearing effect in negligible. The effect of well resistance is neglected. Thus the factor *F* (Equation 5.12) which is a function of drain spacing, smear, and well resistance is converted to the following equation (5.12):

$$F = F(n) = \ln\left[\frac{D_e}{d_w}\right] - \frac{3}{4} \quad \text{.....(5.12)}$$

Coefficient of consolidation of horizontal flow can be evaluated by the equation 5.13.

$$c_h = \frac{D_e^2 F}{8t} \cdot \ln\left(\frac{1}{1-\overline{U}_h}\right) \quad \text{.....(5.13)}$$

Taylor's curve fitting method (presented in Section 2.4) has used to determine time of 90 % consolidation, Coefficient of horizontal permeability has evaluated by the Equation 5.14.

$$k_h = \frac{c_h \cdot \gamma_w}{M_s} \quad \text{.....(5.14)}$$

5.4 Results and discussion

For this study five samples from different places have been tested. First three tests have been performed to develop and to readjust the VD oedometer. The fourth test has been performed with vertical drain on undisturbed soil sample from Vanttila (Test No: 4401vd). Incremental oedometer test with vertical drainage (No: 4402k) to evaluate indirectly vertical permeability characteristics, and also falling head permeability test have been performed at different stress level on Vanttila clay.

The samples tested are presented below:

- Remoulded clay from Lahti Karisto. Nº: 4389vd
- Remoulded clay from Lahti Karisto. Nº: 4390vd
- Remoulded clay from Hyvinkää. Nº: 4391vd
- Undisturbed sample from Vanttila. Nº: 4401vd
- Undisturbed sample from Vanttila. Nº: 4402k

The sample was collected from Vanttila from a depth of about 4.94 - 4.99 m. Natural water content of the sample is 75.8 % with 100 % degree of saturation. Initial void ratio is 1.83. Horizontal permeability characteristic of Vanttila have been evaluated with VD oedomter (Test no:4401vd). To avoid uncertainties and to make comparison samples from the same depth have been tested with normal oedometer test (4402k). Taylor's curve fitting method has been used to evaluate coefficient of vertical

permeability (Chapter 2, Section 2.1). Also direct permeability has been measured using modified oedometer (Chapter 2, Section 2.1.6).

A summary of the test performed is presented below:

1. Indirect evaluation of vertical permeability with normal vertical oedometer using Taylor's method (Test no 4402k)
2. Direct vertical permeability results (Test no 4402k)
3. Indirect evaluation of horizontal permeability using VD oedometer (4401vd)

Horizontal permeability – relative compression relationship obtained in the VD oedometer is presented in Fig 5.6. Coefficient of horizontal permeability k_h are $4*10^{-9}$ m/s to $1.1*10^{-9}$ m/s for relative compression 3.15 % to 23.92 % respectively. In logarithm k_h – relative compression curve the relationship is approximately linear from strain 3.15 % to 23.9 %. At 29.5 % coefficient of horizontal permeability k_h $4.6*10^{-10}$ m/s and shows non-linearity (Fig 5.6). Tavenas *et. al.*(1983a, 1983b) found that for strains up to 20 % a linear relationship exists between the void ratio and logarithm k_h.

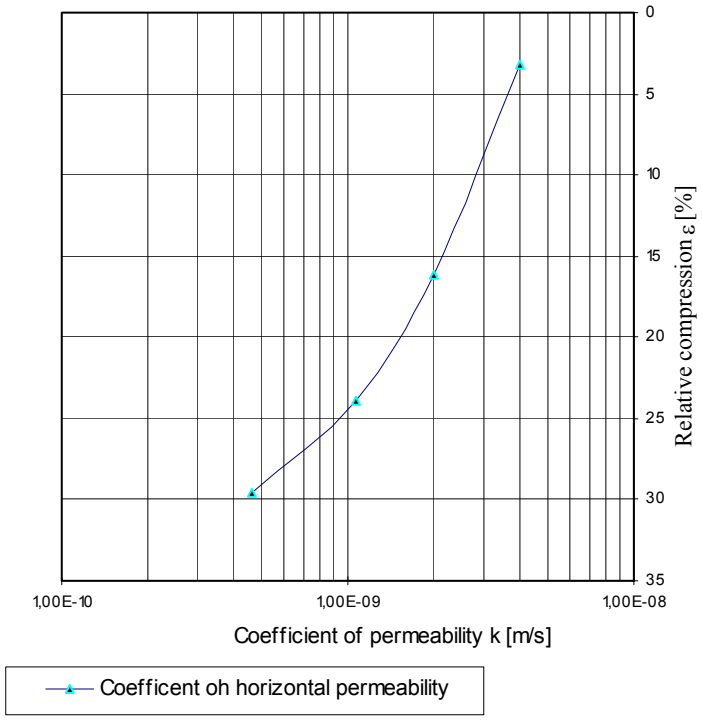

Figure 5.6: *Coefficient of horizontal permeability vs relative compression (Vanttila, 4401vd)*

In Fig 5.7, Coefficient of vertical permeability k_v – relative compression results are presented. Coefficient of vertical permeability k_v evaluated by Taylor's method are $1.46*10^{-9}$ to $2.19*10^{-10}$ m/s for relative compression from 2.2 % to 18.8 % respectively. Whereas, directly measured coefficient of vertical permeability k_v are $2.9*10^{-9}$ to $8.1*10^{-10}$ m/s for relative compression from 2.8 % to 21.6 % respectively. In logarithm k_h – relative compression curve both the methods show approximately linear relationship, though slopes β_k of Taylor's method and direct measurement are 3.60 and 2.98 respectively. Generally, direct measurement of coefficient of vertical permeability k_v is higher than indirect evaluation. In this case, direct measurement is approximately 2 times higher at the beginning than Taylor's method, but it becomes approximately 3.7 times higher with increasing strain.

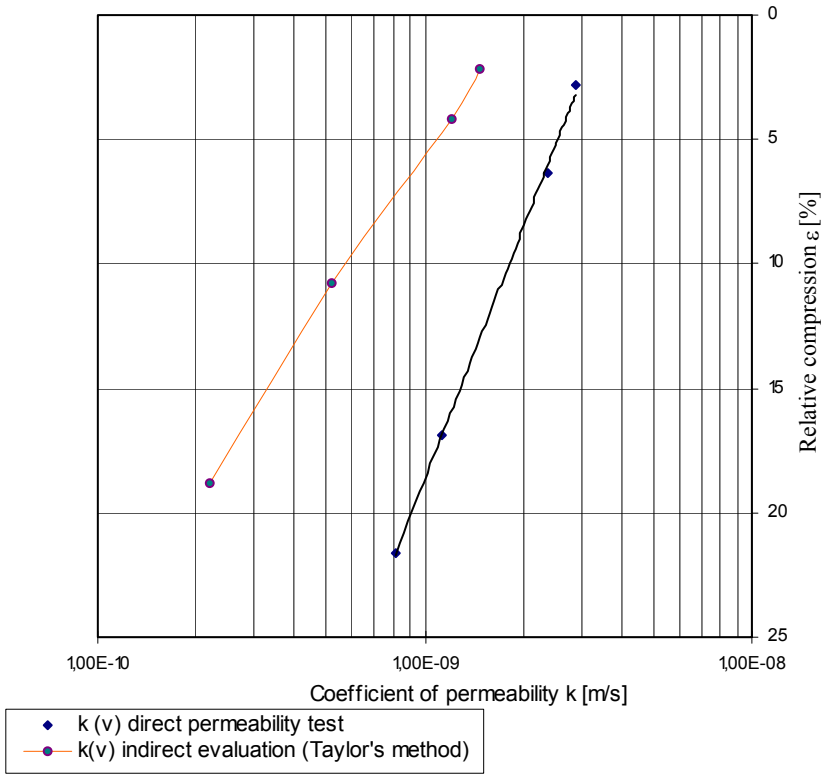

Figure 5.7: *Coefficient of vertical permeability vs relative compression (Vanttila, test no 4402k)*

Estudillo (2003) compared direct measurement and indirect evaluation of coefficient of vertical permeability of three different places Murro, Hyvinkää and Fallkulla of Finland of depth about 10 m, 2.66 m, and 6.3 m respectively. Indirect evaluation of vertical permeability by Taylor's and Casagrande's methods were much lower than

from direct oedometer measurement and Casagrande's vertical permeability values were more dispersed.

Generally, approximate ratio of direct measured vertical permeability and indirect evaluation by Taylors's method depends on sample geotechnical characteristics and vary between 2 to 4. Estudillo (2003) found out the vertical permeability ratio of those three places, presented in Table (5.1).

Table 5.1 *Ratio of $k_{oedometer}$ values with k_{Taylor} values (k_{oed}/k_{Taylor}) Estudillo (2003)*

	Murro	Hyvinkää	Fallkulla
Natural clay	3	3	4
Remoulded clay	2	3	4
Slurry	2	1,8	-

Comparison between coefficient of vertical permeability k_v (directly measured) and coefficient of horizontal permeability k_h is presented in Fig 5.8. Coefficient of horizontal permeability k_h is higher than coefficient of vertical permeability k_v. In logarithm k_h – relative compression both methods shows linear relationship up to strain more than 22 % and approximately same β_k value. The horizontal to vertical permeability ratio is 1.36 approximately up to this limit.

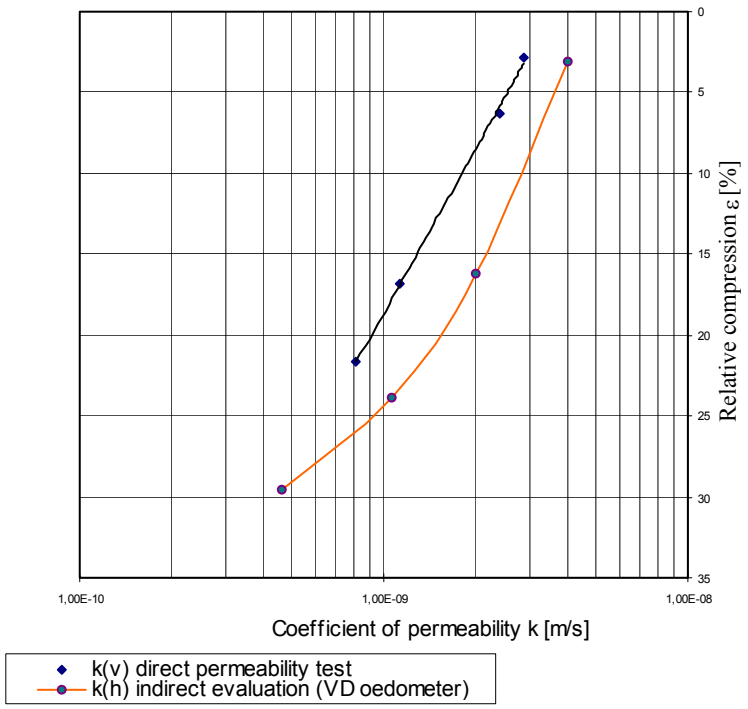

Figure 5.8: *Coefficient of permeability vs relative compression (Vanttila, test no 4401vd & 4402k)*

Leroueil *et.al.*(1990) showed permeability characteristics of seven different clays from five different sites. Four of those sites are Lousieville, Saint-Alban, Saint-Esprit, Matagami from Canada and Bäckebol locates on the Swedish west coast. Permeability measurements were performed using oedometer, triaxial and radial-flow permeameter. Lousieville sample, which was from 9.2 m depth, showed permeability ratio r_k 1.35 to 1.55 from high void ratio to void ratio 1. Saint-Esprit samples were from 5.9 m depth and 9.2 m depth, had permeability ratio 1.15. Bäckebol sample was from 4.3 m depth, showed permeability ratio from 1.88 to 1.33. Though Vanttila clay permeability ratio is 1.36 and VD oedometer provides promising results but it cannot be concluded based on only one test that VD oedometer will provide authenticated results.

Water content profile of Vantila clay (4401vd) after test is presented in Fig. 5.9. Variation in water content of the sample is small. The top part of the sample shows higher water content than the bottom part. This may be because of leakage or displacement of the insulation during the test. One of the main concerns of this test is the friction between the sample and the ring. Though water content variation is small but it cannot be concluded that the friction developed during the test is insignificant. The initial water content of the sample was 75.8 %. The initial water content represents average water content of the sample. According to 'equal strain theory', excess water expelled out should be same from all differential cube of the sample. The variation in water content after test is approximately 13.3 %. Water expelled out from the sample was not uniform because of leakage or displacement of the insulation and friction between the sample and the ring. Because of this phenomenon it can be concluded that the load distribution was uniform during the consolidation phase. Therefore, validity of 'equal strain theory' in this case is a coarse approximation of the actual behaviour.

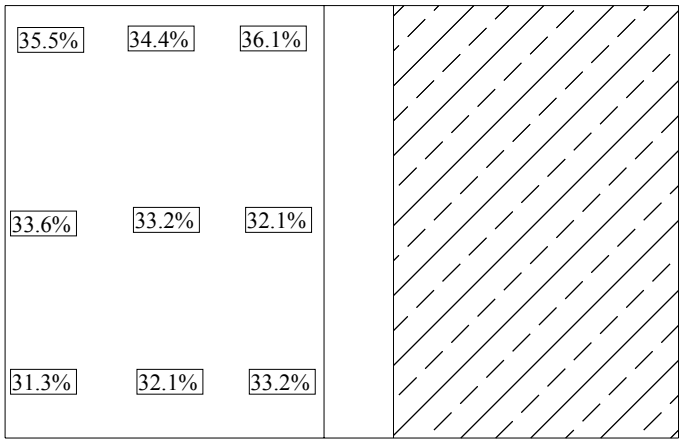

Figure 5.9: *Water content of the sample after test (4401vd)*

To avoid uncertainties associated with the natural variability of clays on the evaluation of permeability anisotropy the following points are recommended

1. Sample trimming: To avoid outside disturbance during trimming care should be taken.
2. Mounting procedure: As the bottom of the VD oedometer is fixed, sample mounting should be done with extreme care.
3. Improvement of insulation: To test Vanttila clay thin plastic was used. Relatively thick insulation will improve the test.
4. Drain installation: As smear effect couldn't be taken on laboratory testing, drain installation is one of the main concerns. To avoid smear drain should be installed before sample mounting.
5. Water content profile: To get better water content profile before and after test samples from different parts should be tested.

Despite the improvements of the VD oedometer and testing procedure, samples from different sites and from different depths should be tested. To validate VD oedometer permeability characteristics finite element simulation of VD oedometer should be performed and checked. Also indirect evaluation from other tests, direct measurement, and *in-situ* results should be compared.

6. CONCLUSIONS

The first objective of this thesis is to study the deformation behaviour of soft Finnish clay. Construction on natural soft soil deposits is still a challenge in geotechnical engineering. Accurate determination of the consolidation and deformation has important economic consequences. Toukoranta is situated in the eastern part of Helsinki near to the outlet of river Vantaa. The area was considered completely unsuitable for building purposes because of underlain soft soils, thereby served mainly as filling area and the original ground level was below sea more than 1 meter. The City of Helsinki fully reclaimed the area by placing filling material over frozen sea in 1985. The soil deposit is more than 20 m thick and roughly divided into five layers-fill layer, organic clay, clay, silt and sand. The thickness of the soil layers varies from location to location as well as the bottom rock level.

Numerical back-analysis of reclamation and test construction is presented. Filling operation was started around 1963. The area was fully reclaimed from sea in 1985. In FEM calculation, it has been assumed that the reclamation of the whole area is done in a single operation to simplify the calculation. The calculated maximum vertical settlement from 1985 to 1995 is approximately 1130 mm. Vertical settlements are approximately uniform and more than 1000 mm of the whole area and pore pressure dissipation is found low because of low permeability and drainage path. After the test construction in 1995, horizontal deformation was main concern. Horizontal movements were measured from December 1995 to February 1996. Calculated and observed maximum horizontal movement of inclinometer 651 are 101 mm and 93 mm. Calculated and observed horizontal movements of other inclinometers agreed fairly well for clay layers. Discrepancy found between the calculated and observed horizontal displacements at the fill layer and inclinometer 652 showed approximately -26 mm displacement at the formation ground level, contrary calculated displacements is 13 mm. Material properties of the fill layer is assumed constant but in reality it may vary from location to location. Despite the close agreement between the calculated and the observed horizontal displacements for that small time frame, further investigation of long term observation of pore pressures, settlement distribution, and horizontal displacements with 3D FM analysis are viable.

Second objective of this thesis is to study the horizontal permeability characteristics of soft Finnish clay. Most natural soft-clay deposits are more-or-less anisotropic with respect to their flow properties. Typically, the horizontal permeability or flow is higher than that for flow in the vertical direction. Laboratory determination of horizontal permeability has been presented. Direct measurement of permeability characteristics is better than indirect evaluation. Estudillo (2003) showed that indirect evaluation of vertical permeability characteristics using Taylor's method provides better results than Casangrande's method. Direct measurement of coefficient of vertical permeability k_v was 3 to 4 times higher than indirect evaluation (Taylor's method) for undisturbed soil sample of three sites of Finland having different geotechnical characteristics.

VD oedometer has been developed to simulate 'equal strain' consolidation process based solely on horizontal flow. Geotextile has been used as drain because of high permeability and compressibility. Friction between the oedometer ring and soil is unknown and smear effect is ignored for laboratory testing. Coefficient of horizontal permeability k_h of Vanttila clay, depth of about 4.95 m, are $4*10^{-9}$ to $1.1*10^{-9}$ m/s for relative compression 3.15 % to 23.92 % respectively. The ratio of indirectly evaluated horizontal permeability to directly measured vertical permeability is found 1.36. Shortcomings in the testing procedure and equipment are mentioned and should be improved for future testing. Further testing and investigations of VD oedometer are needed to get authenticated results and also finite element simulation of VD oedometer, indirect permeability evaluation from other tests, direct measurement, and *in-situ* permeability testing are needed.

REFERENCES

Barron, R.A., 1948. Consolidation of fine-grained soils by drain wells. Transaction ASCE, 113, 718-742.

Buisman, A.S.K., 1936. Results of long-duration settlement test. Proceedings 1st International Conference on Soil Mechanics and Foundation Engineering, Cambridge, Mass. 1.100-106.

Butterfield, R., 1979. A natural compression law for soils (an advance on e-log p'). Geotechnique 29: 469-480.

Chan, H.T., Kenney, T.C. 1973. Laboratory investigations of permeability ratio of New Liskeard varved soil. Canadian Geotechnical Jouranl, 10:453-472

Estudillo, S., 2003. Permeability of Finnish soft clay and its application in consolidation and impervious barriers. Final Work, Laboratory of Soil Mechanics and Foundation Engineering, Helsinki University of Technology.

Garlanger, J.E., 1972. The consolidation of soils exhibit creep under constant effective stress. Geotechnique 22: 71-78.

Gulin, K., Wikström, R., 1997. Stabilization of horizontal movements in weak organic clay layers. Proceedings of the Fourteenth International Conference on Soil Mechanics and Foundation Engineering, Vol 3, Hamburg, Germany, p. 1689-1692

Hansbo, S. 1981. Consolidation of fine-grained soils by prefabricated drains. Proc. 10th Int. Conf. Soil. Mech. Found. Engg. , Stockholm, Vol. 3, paper 12/22

Hill, R.,1950. The mathematical Theory of Plasticity, Oxford University Press, London, UK.

Holtz, R.D., Jamiolkowski, M.B., Lancellota, R., Pedroni, R., 1991. Prefabricated vertical drains. CIRIA, London, UK.

Janbu, N., 1967. Settlement calculation based on the tangent modulus concept. Soil Mechanics and foundation engineering, The Technical university of Norway, Trondheim.

Janbu, N., 1969. The resistance concept applied to soils. Proceedings of the 7th ICSMFE, Mexico City 1:191-196.

Larsson, R., 1981. Drained behaviour of Swedish clays. Swedish Geotechnical Institute. Report No. 12. Linköping, Sweden.

Leminen. K., Rathmayer, H. 1983. Experinece on horizontal oedometer tests to Determine the parameter c_h. Improvement of Ground. Proceedings of the Eigth European Conference on soil Mechanics and Foundation Engineering. Helsinki 23-26 May 1983. A.A.Balkema, Rotterdam. S.647-651.

Leppänen, M., 1989. The use of geotextile for embankment reinforcement in the filling area in the Bay of River Vantaa, Helsinki (in Finnish). Master's Thesis, Laboratory of Soil Mechanics and Foundation Engineering, Helsinki University of Technology.

Leroueil, S., Bouclin, G., Tavenas,F., Bergeron, L., La Rochelle, R., 1990. Permeability anisotropy of natural clays as a function of strain. Canadian Geotechnical Journal, 27:568-578

Ohde, J., 1939. Zur Theorie der Druckverteilung im Baugrund. Bauingenieur 14 (1939):33/34: 451-458.

PLAXIS V8.2: PLAXIS manual version 8.2.

Ravaska, O., Vepsäläinen, P. 2001. On the stress dependence of consolidation parameters. Proc. of the XV Int. Conf. of Soil Mechanics and Geotechnical Engineering, Istanbul/27-31 August 2001. Vol. 1. A.A. Balkema Publishers Lisse/Abingdon/Exton (PA)/ Tokyo 2001. ISBN 90 2651839 0. ss 251-254

Roscoe, K.H, Schofield, A.N., and Worth, C.P., 1958. 'On the yielding of soils' Geotechnique 8(1),22-52

Roscoe, K.H, and Schofield, A.N., 1963. 'Mechanical behaviour of an idealised 'wet' clay', Proc. European Conf. on Soil Mechanics and Foundation Engineering, Wiesbaden, vol. 1, pp.47-54

Roscoe, K.H, and Burland, J.B.,1968. 'On the generalised stress-strain behaviour of 'wet' clay', in J. Heyman and F.A. Leckie (eds.) Engineering Plasticity (Cambridge University Press), pp.535-609

Scott, C.R. 1980. Soil Mechanics and Foundations. Third edition. Applied science publisher LTD. London. England.

Tavenas, F., Jean, P., and Leroueil, S., 1983a. The permeability of natural soft clays. Part II: Permeability characteristics. Canadian Geotechnical Journal, 20:645-660

Tavenas, F., Leblond, P., Jean, P., and Leroueil, S., 1983b. The permeability of natural soft clays. Part I: methods of laboratory permeability measurements. Canadian Geotechnical Journal, 20:629-644